TEST METHOD DEVELOPMENT FOR EVALUATING THE FREEZE-THAW PERFORMANCE OF SEGMENTAL RETAINING WALL BLOCKS

A Thesis

by

AARON KINDALL HOELSCHER

Submitted to the Office of Graduate Studies of
Texas A&M University
in partial fulfillment of the requirements for the degree of

MASTER OF SCIENCE

December 2006

Major Subject: Civil Engineering

TEST METHOD DEVELOPMENT FOR EVALUATING THE FREEZE-THAW PERFORMANCE OF SEGMENTAL RETAINING WALL BLOCKS

A Thesis

by

AARON KINDALL HOELSCHER

Submitted to the Office of Graduate Studies of
Texas A&M University
in partial fulfillment of the requirements for the degree of

MASTER OF SCIENCE

Approved by:

Chair of Committee, David Trejo
Committee Members, Stuart Anderson
Winfried Teizer
Head of Department, David Rosowsky

December 2006

Major Subject: Civil Engineering

ABSTRACT

Test Method Development for Evaluating the Freeze-Thaw Performance of Segmental Retaining Wall Blocks.

(December 2006)

Aaron Kindall Hoelscher, B.S., Angelo State University

Chair of Advisory Committee: Dr. David Trejo

Segmental retaining walls (SRW), typically constructed along highways, have grown in popularity over the past decade. Manufacturers of SRW blocks have estimated the service life of a properly constructed wall to be approximately 75 years. However, there have been reports of SRW systems failing after only five years in service. Suspected causes of the SRW failures are freeze-thaw damage while exposed to deicing salts sprayed by snow plows from highways.

The current standard test method used for evaluating the freeze-thaw durability of SRW blocks has several drawbacks and does not accurately replicate environmental exposure field conditions. The objective of this research is to develop and assess a new standard test method for evaluating the freeze-thaw durability of SRW blocks that obtains reproducible results and offers sufficient information on the freeze-thaw performance for SRW block manufacturers and state highway agencies (SHAs).

The research completed a preliminary proof of concept test for the new freeze-thaw test method developed using small, commercially available SRW blocks to mitigate potential problems and establish appropriate test parameters. The testing produced results of freeze-thaw degradation that followed the same modes of failure that has been discovered during field evaluations.

After the proof of concept test was completed, a series of freeze-thaw tests were conducted using sets of SHA approved and non-SHA approved SRW blocks. Three

different manufacturers' SRW blocks were evaluated. There was no significant freeze-thaw degradation of any of the blocks after 200 freeze-thaw cycles, so for two blocks, experiments were extended to 400 cycles using a twelve-hour freeze-thaw cycle. The modification of the test did not result in more rapid deterioration of the SRW blocks.

The researchers found that the freeze-thaw durability test method developed herein is beneficial for determining the freeze-thaw performance of the lower quality specified blocks. The test method gives realistic results, which match typical deterioration modes that are common in field settings, in a timely manner. However, the test method for testing SHA quality SRW blocks takes longer times and may not be a reasonable test for such products.

ACKNOWLEDGEMENTS

The author takes this opportunity to acknowledge the excellent academic guidance and financial assistance offered by Dr. David Trejo during the entire research project. Without his helping hands, this thesis would not have been in its current shape. The support offered by Dr. Stuart Anderson and Dr. Winfried Tiezer is also appreciated. The author offers a special acknowledgement of appreciation to the Federal Highway Administration (FHWA Project No. DTFH61-02-R-00078) for funding the research project.

The author acknowledges all of the technical assistance he received from Mr. Radhakrishna Pillai, Dr. Ceki Halmen, Mr. Adam Frerich, Mr. Brett Halfmann and other members of the Trejo Research Group. Also acknowledged is the help offered by Mr. Duane Wagner, Mr. Lee Gustavus, and other employees of the Texas Transportation Institute.

I greatly appreciate all of the favors and advice I received from my friends including Kelly Donnell, Shane Halfmann, and Matt Schmitt during the course of my graduate studies at TAMU. I offer special thanks to my parents Galen and Leslie Hoelscher and Ronnie and Kay Halfmann for their patience and silent support without which this endeavor would not have been accomplished. Support from other family members is also appreciated. I thank my fiancé Amber Dryden for giving extra support during the final stages of this project. Most of all, I would like to dedicate this report in the memory of my friend, co-worker, and fellow student Mr. Michael Gamble.

TABLE OF CONTENTS

Page

Page

LIST OF FIGURES

Page

Page

Page

LIST OF TABLES

Page

1. INTRODUCTION AND OBJECTIVE

1.1 RESEARCH BACKGROUND

1.1.1 Problem Statement

Segmental retaining walls (SRW), typically constructed along highways, have grown in popularity over the past decade. Because these structures are relatively new to the transportation industry there has been limited research performed on the durability and service life of the SRW block systems. Manufacturers of SRW blocks have estimated the service life of a properly constructed wall to be approximately 75 years [1]. However, there have been several reports of SRW systems failing after only five years in service [1]. Most of the SRW system failures have been in the northeastern United States. Suspected causes of the SRW failures are exposure to freeze-thaw cycles and deicing salts.

1.1.2 Segmental Retaining Walls

SRWs are constructed systems of interlocking blocks used for facing soil retaining walls. These walls are either constructed with a straight vertical face or with a stepped face that changes with a range from 3 to 15 degrees from vertical. A typical SRW along a roadway is shown in Figure 1.1.

This thesis follows the style of the *ASTM Journal of Testing and Evaluation.*

Figure 1.1 Typical SRW located along a roadway [2].

There are several advantages to using SRWs instead of traditional cast in place concrete walls. SRWs can be constructed in almost any location or wall layout because of the wide varieties of size and geometry of SRW blocks. The cost of constructing an SRW is approximately one-half to one-third the cost of other methods [3]. The construction of an SRW is much faster than conventional cast-in-place concrete because formwork or bracing is not required for the SRW systems. Also, the SRW block market offers many different sizes, shapes, and colors of blocks that provide unique architectural designs. However, if freeze-thaw damage occurs, the aesthetic qualities and wall integrity can be lost.

1.1.3 Segmental Retaining Wall Blocks

SRW blocks are classified as a dry concrete product that has a stiffer mixture consistency than that of conventional concrete mixtures. However, the mixture must

contain sufficient water to ensure that the cement paste is mixed throughout the concrete mixture. SRW blocks are manufactured by an automated production method consisting of mixing the construction materials in large mixers, moving the SRW mixture into molds, consolidating the constituent materials in these molds, and then curing the demolding blocks. Typically, the manufacturers mixture design contains Type I portland cement, fine aggregates, water, and if needed supplementary cementitious materials (SCMs). The molds used can vary in size and shape; some blocks are cast with hollowed out sections while others are solid.

The concrete mixture is placed into the molds and then compacted using vibration. After consolidation the blocks are removed from the molds and placed in a curing chamber with an elevated temperature and high relative humidity for approximately twelve to twenty-four hours. SRW blocks can be produced to obtain sufficient early strength in these manufacturing plants, resulting in reduced manufacturing times [3]. A typical production line for SRW blocks is shown in Figure 1.2.

Figure 1.2 Typical SRW block production line [3].

Unfortunately, some SRW blocks have experienced a lack of freeze-thaw durability when exposed to freezing and thawing conditions and deicing solutions. One major difference between SRW blocks and conventional cast-in-place concrete is that SRW blocks are known to contain a continuous network of large compaction voids due to their production process and low water-to-cement ratio [3]. These voids are typically non-symmetric with angular tendencies unlike the spherical voids found in air-entrained concrete used to reduce freeze-thaw damage. SRW blocks are thought to be damaged by freeze-thaw conditions when the compaction voids absorb water at above freezing temperatures and later freeze, converting the water to ice and causing volumetric expansion. The expansion of the water causes an internal pressure on the void walls, forcing the concrete material into tension and leading to the formation of microcracks throughout the block. Microcracks tend to migrate further through the interior of the block with each successive freeze-thaw cycle, reducing the integrity of the structure.

1.1.4 Current ASTM Standard Test Method

Several methods for assessing freeze-thaw durability of concrete and masonry units have been developed over the years. The current standard test method for evaluating the freeze-thaw durability of dry-cast SRW units is ASTM C 1262, *Standard Test Method for Evaluating the Freeze-Thaw Durability of Manufactured Concrete Masonry Units and Related Concrete Units* [4]. This method consists of subjecting cut portions of SRW block specimens to freeze-thaw cycles. The SRW block specimens can be either partially or fully immersed in pure water or saline solution in a single container. After twenty-five freeze-thaw cycles, the samples are removed from the containers and rinsed with water to dislodge the loosened particles. The particles are then filtered from the rinse water and weighed. The amount of block deterioration is calculated by dividing this weight by the saturated weight of the specimen. Block failure is determined when the accumulated loosened or scaled particles exceed ten percent of the saturated weight of the specimen or the experiment is abandoned after 500 freeze-thaw cycles are completed [4]. The standard test set-up for the ASTM C 1262 test is shown in Figure 1.3.

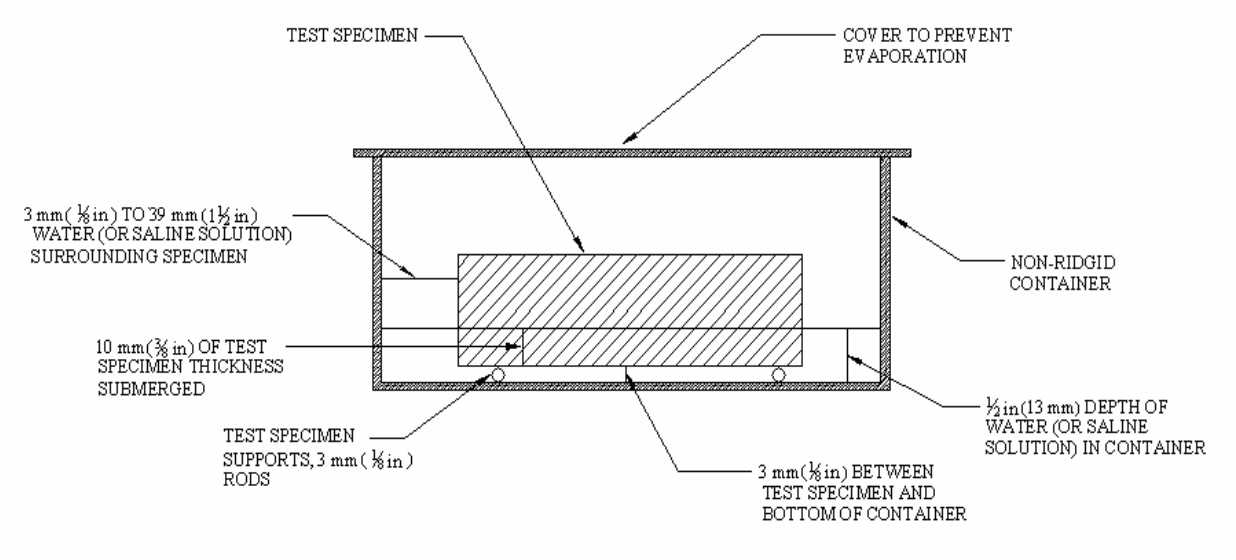

Figure 1.3 Test set-up for ASTM C 1262 standard test method [4].

Several problems are evident with the ASTM C 1262 test method. The test method does not accurately depict real-life freeze-thaw environmental conditions and the specimens are immersed in water or saline solutions which is generally not typical of SRW systems in the field [4]. Also, ASTM C 1262 does not specify standard rates of freezing and thawing during the test procedure nor does it define temperature hold times for the samples [4]. This standard test method incorporates very aggressive freeze-thaw cycles that may not replicate thermal conditions that are present in the field. The method specifies that as soon as the center section of the SRW block reaches freezing temperatures, the thaw cycle can begin and then when the center of the block is thawed the temperature should be reversed. This aggressive cycling is specified to minimize the testing time. However, extensive freeze-thaw damage occurs when a rapid decrease in temperature takes place. Usually, in field situations a time period of two to three hours is required to reach freezing conditions.

SRW blocks tested in the lab exhibit significantly different damage than SRW blocks exposed to field conditions. By slowing the rate of the testing process,

mechanisms of deterioration similar to that in the field can be obtained. Without controlling these specification requirements, researchers typically obtain large variations in the results due to the ill-defined test procedure. Also, when different freeze-thaw chambers are used, their system capabilities vary, causing variability in the test results.

Another potential drawback of the test is that the specimens in the ASTM C 1262 test method are cut portions of a single SRW block [4]. By cutting the specimens, usually from the back side of the block, representative damage to the front of the blocks, where freeze-thaw and chloride induced damage is most likely to occur in the field, is not assessed. Also, specimens are placed separately in a freeze-thaw chamber instead of a wall system where several SRW blocks are grouped together. By grouping the SRW blocks in a simulated wall setup, more accurate field deterioration are likely to be achieved because stresses caused by adjacent blocks and drainage typical of that found in the field can be simulated. Thus, a new test method that represents field conditions is needed so that state highway agencies (SHA) and manufacturers can better assess the freeze-thaw durability performance of SRW blocks.

1.2 RESEARCH OBJECTIVE

The research described in this report was performed as a part of Federal Highway Administration (FHWA) Project DTFH61-02-R-00078 study on the durability of SRW blocks. The funded study is a collaborative effort involving research performed at the University of Texas, Cornell University, Vermont Technical College, and Texas A&M University. The work presented in this report was conducted primarily at Texas A&M University.

The objective of this research is to develop a preliminary proof of concept test set-up for evaluating the freeze-thaw durability of SRW blocks that result in reproducible results and offers sufficient information to SRW block manufacturers and SHAs. The research study at Texas A&M University will complete the following tasks to fulfill the objective.

1. Conduct a literature review to identify freeze-thaw failure modes and test method techniques for SRW blocks.
2. Perform material characterization of SRW blocks consisting of microscopy and a diffusion coefficient determination of the SRW blocks.
3. Develop and evaluate a new standard test method that represents the freeze-thaw field performance durability of SRW blocks.
4. Perform proof of concept and preliminary laboratory investigations on samples received from manufactures to assess the replication of field freeze-thaw damage modes using the new test method.

The literature review consisted of reviewing pertinent background information on SRW blocks and systems along with recent studies of freeze-thaw field assessments and laboratory experiments on SRW blocks. Literature addressing typical mechanisms of freeze-thaw damage, internal pore structures, and microcracking in concrete, along with SRW blocks, have been reviewed. Also, research on previous freeze-thaw durability test methods in conjunction with other testing techniques that could be helpful in developing a new test method was investigated.

Material characteristics were assessed from experimental procedures completed at the University of Texas and Cornell University. SRW blocks are from the same batch of blocks being tested in the freeze-thaw chambers were used at all participating universities. Material characteristics evaluated included compressive strength, modulus of elasticity, absorption, and density.

Microscopy work was completed as part of the research at Texas A&M University. In addition, prior to testing blocks in the new freeze-thaw chamber, the diffusion coefficient was determined to provide information on the rate at which chloride ions are transported into the SRW block samples. These data were used to assist the

researchers in determining how chloride ions influence the freeze-thaw performance. Comparisons with similar materials can then be made.

After conducting the literature review and the material characterization, a new preliminary standard test method was developed. The basis of this new preliminary method was to better replicate actual freeze-thaw field environments in a laboratory setting while minimizing test time. The new method specifies temperature gradients in addition to hold times at the maximum and minimum temperatures during the test. The researchers realize that the geometry and size of SRW blocks vary, but believe a standard test procedure is feasible. Wall systems containing SRW blocks were tested to represent an actual wall in the field. Also, saline or fresh water solutions were sprayed on the test samples instead of immersing the samples to better replicate field conditions.

Attempts were made to design the test method to be easy and relatively inexpensive to perform and offer timely, satisfactory test results. The method was designed with the hopes of providing SHAs and SRW block manufacturers with sufficient information to compare the quality and freeze-thaw durability of blocks that are currently on the market in the United States.

The fourth task of the research was to perform laboratory investigations on samples to assess the field freeze-thaw damage performance using the new preliminary test method. Small, commercially available SRW blocks and large SRW blocks used by SHAs were evaluated. By implementing the new preliminary method, the results of the freeze-thaw test were compared to the results of the ASTM C 1262 test method [4]. Several different freeze-thaw damage data collection techniques were used to analyze the freeze-thaw deterioration of the SRW blocks. This was performed to provide evidence of SRW block failure. These methods include mass loss measurements, visual inspections, and microcrack assessment.

1.3 SCOPE OF REPORT

This report contains six sections. The second section of this report is a discussion and synthesis of the current literature to identify freeze-thaw failure modes and test

methods for SRW blocks. The third section identifies and explains materials and presents a new preliminary test setup and test methodologies used for assessing freeze-thaw damage and durability of SRW blocks. The fourth section of this report explains the experimental design developed to perform the necessary experiments to fulfill the research objectives. The fifth section offers an analysis of the results from each evaluation made during the course of the research. Section six provides a summary of the research, conclusions, and recommendations for future research.

2. LITERATURE REVIEW

A literature review was completed to identify and review pertinent background information regarding SRW blocks and systems along with recent studies of freeze-thaw field assessments and laboratory experiments on SRW blocks. Literature addressing typical mechanisms of freeze-thaw damage, internal pore structures, and microcracking in concrete, along with SRW blocks has been reviewed. Also, research on previous freeze-thaw durability test methods in conjunction with other testing techniques that will be helpful in developing a new test method has been investigated.

It was first necessary to develop an inclusive understanding of the microstructure and freeze-thaw mechanisms of conventional concrete because extensive studies pertaining to this material are available in the literature. With knowledge of the important components that relate to the freeze-thaw performance of conventional concrete, comparisons can be made with the microstructure and freeze-thaw mechanisms of SRW blocks. This review provides a background on the mechanisms present in SRW blocks subjected to moisture and freeze-thaw conditions that assisted in the development of the new preliminary test method for investigating the freeze-thaw performance of SRW blocks.

2.1 CONVENTIONAL CONCRETE MICROSTRUCTURE AND FREEZE-THAW MECHANISMS

Conventional concrete has a very heterogeneous and complex microstructure consisting of hydrated cement paste, coarse and fine aggregates, gel pores, capillary voids, air voids, supplementary cementitious materials (if used), along with any additional chemical additives. There is some inconsistency found in typical concrete structures; some areas of the hydrated cement paste are extremely dense while other areas are porous, the aggregates' geometry varies in shape and size, and the capillary and air void system is often random, unless air-entrainment is used.

The hydrated cement paste is the paste made when combining portland cement and water. When portland cement is dispersed in water, its components rapidly scatter and chemical reactions cause several different crystal structures to form and position themselves throughout the paste. The various phases of these crystals are neither uniformly distributed, uniform in size, nor morphologically similar [5]. This lack of microstructural homogeneity can have to major effects in the physical properties of this material.

Some portland cement particles are anhydrous particles which, when mixed with water, tend to attract each other, causing local variations in the water-cement ratio. This variation is one primary source of the heterogeneous pore structure. With highly condensed masses suspended in the cement paste system, the size and shape of pores, as well as the crystalline products of hydration, are known to be different when compared to well-dispersed systems [5].

The three basic types of pore systems present in hydrated cement paste are the gel pores, capillary voids, and air voids that are defined by their size. The smallest voids are gel pores that have a radius of 1 nm (0.04×10^{-6} in) or less. The irregularly shaped capillary voids are the spaces not taken up by the cement or the hydration products. These voids are formed because the volume originally occupied by the cement and water remains essentially unchanged during the hydration process. Large capillary voids are considered to be larger than 50 nm (2×10^{-6} in), which are assumed to be unfavorable for the strength and impermeability, while small capillary voids are smaller than 50 nm (2×10^{-6} in) and have been reported to affect drying shrinkage and creep [5]. Both gel pores and capillary voids contain water depending on the environment that the concrete is located. The larger capillary voids are important to freeze-thaw performance because they contain free water, which when frozen, can exert pressure on the surrounding cement paste.

Setzer investigated the mechanics of the condensation and suction of three different pore water types [6]. He then classified the different pore sizes and identified the type of water that is present in each. This is summarized in Table 2.1.

Table 2.1 Pore size, classification, and pore water.

Pore Class	**Upper Radius**	**Kind of Water**	**Filled By**
Micro gel pores	1 nm (0.04×10^{-6} in)	Structured	Sorption (<50 percent relative humidity)
Meso gel pores	30 nm (1.2×10^{-6} in)	Prestructured	Vapor condensation (50 to 90 percent relative humidity)
Micro capillaries	1 μm (39.4×10^{-6} in)	Bulk	Suction (no max height)
Meso capillaries	30 μm (12×10^{-4} in)	Bulk	Suction (max height reached after minutes)
Macro capillaries	1 mm (0.04 in)	Bulk	Suction (max height reached below one minute)

The largest of the voids in concrete are entrapped air voids. These voids are typically irregularly shaped. Entrapped air voids form during the mixing process, while entrained air voids are a result of using chemical admixtures. Entrapped air voids can be as large as 10 mm (0.4 in), while entrained air voids usually vary in size of 50 to 200 μm (0.002 to 0.008 in). These air voids are in general much larger than the capillary voids. A polished cross-section of air-entrained concrete as seen through a microscope is illustrated in Figure 2.1.

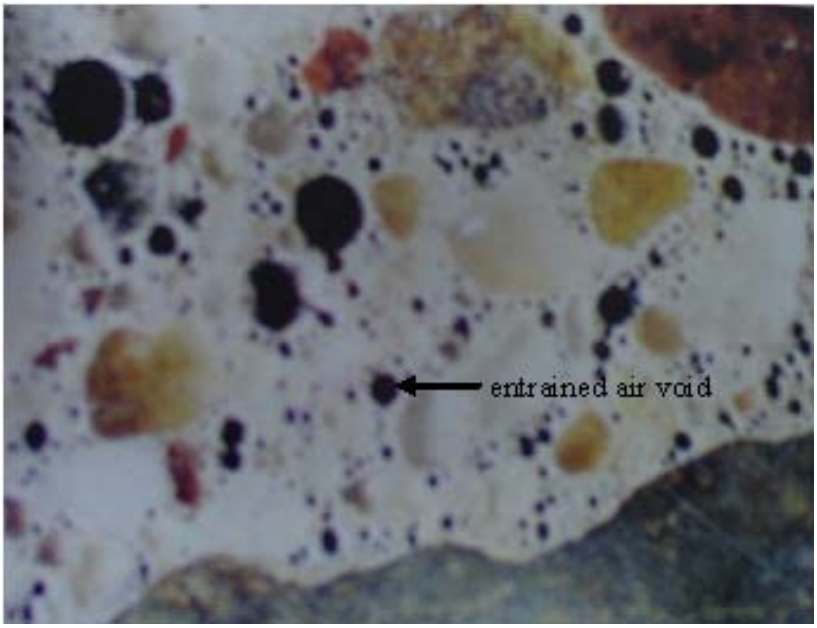

Figure 2.1 Polished section of air-entrained concrete as seen through a microscope [7].

Entrained air can be introduced into a concrete using a variety of surface-active chemical compounds. These compounds, also known as surfactants, typically contain a nonpolar hydrocarbon chain. These nonpolar hydrocarbon chains form at the void-water interface causing these voids to be separated by a distance of 0.1 to 0.2 mm (0.004 to 0.008 in) [5]. In addition, the positive surface charges on the cement grains tend to attract the negative surface charges on the entrained void. This distribution of charges in the hydrating cement paste result in the formation of an evenly distributed, relatively uniformly sized entrained air void system. This air void system provides relief valves throughout the concrete microstructure, making the concrete resistant to cracking and damage typically associated with the volume increase associated with freezing pore water. It is thought that air entraining admixtures cause the inside spherical surface of the air-entrained voids to become hydrophobic. The hydrophobic characteristic repels the water forced into the air-entrained voids during freezing conditions back to the capillary voids so saturation, when not under freezing conditions, is not achieved.

2.1.1 Hydraulic Pore Pressure due to Freezing Water

The most evident mechanism of freeze-thaw related damage to cementitious materials results from internal hydraulic pore pressures that exists when the internal water freezes. When water freezes, a nine percent volume increase is achieved. This increase causes hydraulic pressures unless the unfrozen freezing water can move from the void via escape routes [8]. Saturated specimens cooled below freezing temperatures form amorphous ice crystals when the water is frozen and will reduce the ability of some of the free water to exit the capillaries [9]. The hydraulic pressure may vary according to the distance to the escape routes, permeability of the concrete, and the rate of temperature change. When hydraulic pressures are present, tensile stresses will form on the surrounding cementitious material and initiate microcracking. Figure 2.2 shows typical cracking of conventional concrete due to freeze-thaw exposure.

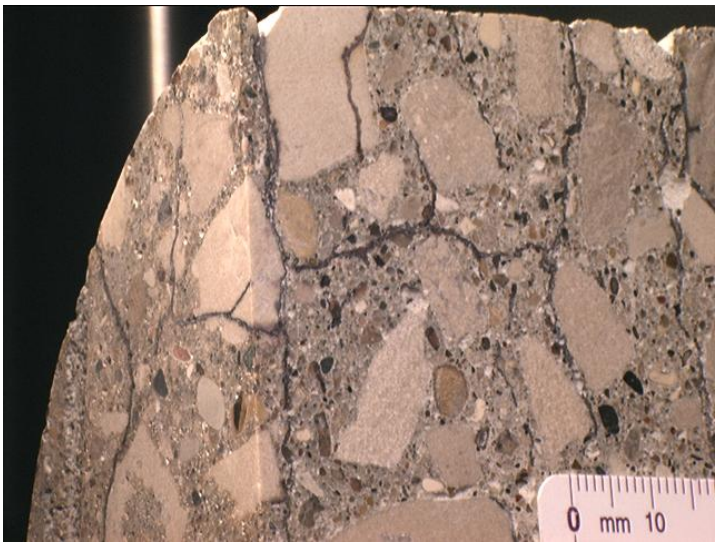

Figure 2.2 Typical cracking of conventional concrete due to freeze-thaw damage [10].

Powers and Litvan both suggested that the pore water moves away from freezing conditions through escape routes caused by expansion of frozen water [8,9]. However, Collins suggested the frost damage mechanism is driven by thermodynamic equilibrium

between ice and water [11]. His study indicated that ice segregates into lenses while freezing and the free water actually moves towards the frozen areas. The damage is then caused by the growth of the ice crystals as more water freezes. This growth initiates internal pressures to cause microcracking and freeze-thaw damage. Powers revised his initial theory after he found that partially dry, non-air-entrained cement paste will shrink and then expand when frozen [12]. This held true also when the temperature was held constant. Also, with the same conditions present, air-entrained cement paste will continue to shrink. Powers also noticed that freeze-thaw damage could occur in specimens that contain liquids with little expansion when frozen. These findings led him to support the theory that water is actually moving towards the freezing locations.

Setzer reported on the freeze-thaw behavior and the influence of deicing chemicals for the three types of pore water (structured, prestructured, and bulk or free) [6]. The structured and prestructured pore water is found in gel pores, while the bulk or free pore water is found in capillary and air voids. The freezing of the pore water is depressed due to the interaction with the internal surfaces of the hydrated cement paste. The freezing point decreases exponentially from a radius of 16 nm (6.4×10^{-7} in) at -9°C (15.8°F) to 3 nm (1.2×10^{-7} in) at -45°C (-49°F). After exposing deicing chemicals to concrete blocks, the freezing points were shifted. Setzer found that the phase transitions of the prestructured gel pore water broadens and flattens out with increasing salt concentration. These prolonged phase transitions are thought to contribute to more extensive freeze-thaw damage. The researcher also found that as salt concentration of 3 percent is the most detrimental for freezing because much of the pore water freezes above -20°C (-4°F).

2.1.2 Thermal Expansion of Aggregates and Cementitious Materials

Freeze-thaw damage can also occur in cementitious materials resulting from thermal incompatibility of the constituent materials. When the thermal expansion coefficients differ between the materials in a concrete mixture, the materials expand and contract at different rates when subjected to temperature variations. This difference

causes tensile stresses at the boundaries between the materials, which lead to cracking of the concrete [13]. The cracks will continue to progress causing more extensive damage to the concrete. Also, popouts, small flakes, or chips of concrete expelled from the surface are likely the result of thermal mismatch between the individual aggregate particles located near the surface and the hydrated cement paste [1].

Fagerlund conducted an experiment to examine the effect of the inner salt concentration, and the effect of the degree of salt water saturation on the expansion of a specimen during a single freezing [14]. The samples were then saturated with the NaCl solutions by applying a vacuum for three months so that the pore water at the center of the specimens would reach equilibrium with the outer edges. The samples were immersed in kerosene and the temperature was decreased to -28 °C (-18.4 °F). The simultaneous ice formation and sample length change was measured.

The researcher concluded that when the level of saturation was low, no or very little expansion occurred for all salt concentrations. However, at high levels of saturation, the largest expansion occurs with a 2.5 percent NaCl solution. The researcher also verified that 5 and 10 percent concentrations were not more harmful than pure water.

2.1.3 Salt Scaling

Researchers have also investigated the effect of exposing concrete to deicing solutions. These solutions were investigated because the standard deicing treatment for roadways in the United States is to spray bridges and roadways with a saline solution before or during freezing conditions. The saline solution lowers the freezing temperature of the surface water to retain traction characteristics. However, the use of deicing salts has been proven to be associated with additional deterioration of concrete structures [11].

When deicing salt solutions are applied to cementitious material systems, these solutions can delay the evaporation of water, prolonging the saturation period. The unfrozen water throughout the concrete is then attracted toward the surface where it can not escape because of ice formations on the surface [15]. The trapped water creates internal pressure pushing on the outer layer which causes scaling. It was found that no surface scaling existed when there is no salt layer or if the layer was replaced by fresh

water [16]. Pigeon and Langlois found that the resistance to deicing salt scaling increased when water-cement ratios are less than 0.30 [17]. Bilodeau and Malhotra concluded that salt scaling resistance of concrete is strongly influenced by the quality of the concrete and air-void structure at the surface [18].

Salt scaling was the most severe when samples were tested with a NaCl solution with an outer salt concentration of 2.5 percent for air-dried samples, and 5 to 10 percent for specimens stored in water before the test [14]. Also, when the air-entrained content of the concrete was increased, the salt scaling resistance was increased [14].

2.2 CONVENTIONAL CONCRETE FREEZE-THAW MATERIAL PARAMETERS

It is important that this research identify the affects of different influencing parameters for conventional concrete mixtures and they evaluate if these parameters influence the performance of SRW blocks. This information can provide the readers with a basic understanding of the methods that are used in conventional concrete to protect against freeze-thaw degradation so that they can use this background knowledge to assess the freeze-thaw performance of SRW blocks.

2.2.1 Supplementary Cementitious Materials

SCMs are often added in concrete mixtures for various reasons. Researchers have been interested in the affect of adding admixtures and pozzolans to reduce freeze-thaw degradation. It was discovered that, overall, the use of these materials affected the salt scaling in a negative manner [18]. Janssen and Snyder conducted freeze-thaw experiments on concrete with and without deicing salt exposure using the test method ASTM C 666, *The Standard Test Method for Resistance of Concrete to Rapid Freezing and Thawing* [19,20]. They exposed several concrete samples to repeated freeze-thaw cycles while applying deicing salts or fresh water to some of the samples. The samples contained air entraining agents and various combinations of water-reducing admixtures, fly ash, and blast furnace slag. The mixtures containing SCMs showed little mass loss,

while those containing 100 percent cement had substantial mass loss. Jacobsen and Sellevold found that concrete mixtures containing silica fume showed significantly less ice formation and less scaling [21].

2.2.2 Air Entraining Admixtures

It is important in freeze-thaw studies of concrete exposed to deicing salts to identify the most suitable amount of air-entrainment for the best performance. Studer performed research to observe frost and deicing salt resistance of concrete [16]. Test specimens were made with three entrained-air contents of concrete that normally would exhibit high, medium, and low durability against freeze-thaw damage and deicing salt scaling. Each sample was covered with a layer of 3 percent NaCl solution during freezing conditions. The air entrained concrete with an air content of 5.2 percent by volume showed the best freeze-thaw resistance, while the concrete with lower air contents was less durable.

2.2.3 Water Absorption

The amount of water absorption by concrete is a key parameter when studying freeze-thaw durability. Fagerlund conducted an experiment to investigate the effect of salt water absorption on air-cured samples versus water-cured samples [14]. For high water-cement ratios, a higher salt concentration resulted in higher degrees of saturation when the air content was low, but lower levels of saturation when the air content was high. This also occurred in the other water-cement ratios, but not as significant. Fagerlund also found that the absorption was higher during freeze-thaw tests when the samples were tested in saline solutions. An explanation for these results is that it is more difficult to fill air entrained pores with salt solutions than pure water. Also, it was found that freeze-thaw situations result in larger absorption quantities concrete samples cured in water. This could be caused by the pores opening, i.e. increasing in size, after the first freeze-thaw damage and allowing more absorption [14]. Greater absorption will in turn create more internal pressures causing further damage.

2.3 CONVENTIONAL CONCRETE FREEZE-THAW TEST PARAMETERS

Before developing a new standard test method for evaluating the freeze-thaw performance of SRW blocks, the researchers evaluated literature pertaining to freeze-thaw test parameters. The main parameters for freeze-thaw testing are temperature ramping rates, freeze-thaw cycle times, and NaCl solution concentration. These variables were investigated to better understand the affects of each and decide on the appropriate value for each to use during the new testing.

2.3.1 Freezing and Thawing Temperature Ramping Rates and Cycle Times

There is evidence that varying freezing and thawing ramping rates along with cyclic exposure times result in different amounts of freeze-thaw degradation of cementitious material systems. Increased freezing and thawing rates can produce more damage because higher rates raise the rate in which water must escape pores and capillaries [9].

Richie and Davison conducted a field study monitoring the temperature changes of cementitious materials at two locations for two years [22]. The variables that were assessed was the geographic location, direction of exposure, season of the year, number of freeze-thaw cycles exposed, and the rate of temperature changes. Several samples were fitted with thermocouples to asses the freeze-thaw cycles and temperature rates.

The freezing conditions were different for the samples facing different directions. Some of the samples never exceeded freezing temperatures, while others experienced significant freeze-thaw cycles. When the thermocouples were moved from the center of the samples closer to the exposed face, more freeze-thaw cycles were measured. The rate of freezing in the natural setting was much slower than the laboratory testing. The cooling rate of the samples normally was 1.1 to 1.7°C (2 or 3°F) per hour with a maximum rate of 5.5°C (10°F) per hour. This rate was suggested to be the maximum rate of freezing for laboratory testing. Also recommended was that more realistic conditions should be used for laboratory freeze-thaw testing.

Stark researched the affect of different cycle exposure times on freeze-thaw damage [23]. The researcher tested samples with freeze-thaw cycles of one per week and two per day. The investigator found that the samples exposed to the longer freeze-thaw cycles experienced much more damage than those subjected to the shorter cycle times. The explanation of this result is that if liquid is attracted to the ice crystals that form in voids and capillaries, the longer the cycle time, the more time the liquid will have to move towards the existing ice [23]. Therefore, more internal pressure will exist as more ice is formed internally.

Setzer completed a series of freeze-thaw experiments on concrete samples using the capillary suction of deicing chemicals and freeze-thaw test [6]. This test method used capillary suction to saturate the samples with the saline solution before the experiment began. The investigator discovered that implementing two freeze-thaw cycles per day versus one freeze-thaw cycle did not significantly affect the results, as long as the minimum temperature was held for three hours. This long hold time ensured that all of the free water present in the concrete microstructure would freeze.

Studer investigated how different types of temperature cycles affected the degradation of concrete exposed to a 3 percent NaCl solution and a freeze-thaw environment [16]. Two of the sample sets were exposed to cycles of -13°C (-55.4°F) to 13°C (55.4°F) and two of the sets were exposed to -20°C (-68°F) to 20°C (68°F). The cycle times varied from 12, 16.8, and 24 hour time periods. The change in temperature ranges showed a significant variation in frost damage of the samples. When the minimum temperature was raised, it caused an increase in the amount of scaling from 38 to 52 percent. When increased again the amount of scaling changed from 4 to 22 percent. However, the duration of the frost cycle, freezing rate, and the temperature-time curve during the thawing phase did not present a discernible influence in this study.

2.3.2 Sodium Chloride Concentrations

When investigating the affects of concrete exposure to NaCl solutions, it is important to understand the results of using different concentrations of saline solutions. Janssen and Snyder [19] conducted an experiment to compare the effect of exposing fresh

water versus a NaCl solution while subjected to freeze-thaw conditions. The samples exposed to fresh water experienced no mass loss, while those exposed to salt solution showed significant mass loss [19].

As already noted, Fagerlund investigated the surface degradation of specimens that were exposed to freeze-thaw conditions completely immersed in different NaCl solutions [14]. It was found that scaling was more prevalent at the lower portions of the samples and that freeze-thaw damage was most severe when exposed to a 2.5 percent NaCl solution. Samples that were water-cured for six weeks and then air dried for two weeks showed that 10 percent NaCl solutions are not much more harmful than freezing in pure water. However, samples that were water-cured for six weeks with only one week of air drying indicated that the 5 and 10 percent NaCl solutions were the most severe. The reason for this behavior is thought to be that the salt migrates in the pores by a slower diffusion process when air dried for one week. It is believed that the inner salt concentration in the mortar is the same for both curing methods, and the 2.5 percent NaCl solution is still the most deleterious.

2.4 SRW BLOCK MICROSTRUCTURE AND FREEZE-THAW MECHANISMS

The low water and cement content and elevated curing temperatures of SRW blocks make the microstructure of these blocks different from ordinary concrete. The dry concrete mixture must have a low enough slump to allow for immediate de-molding and the mixture must contain sufficient cement and water to ensure that this cement paste is distributed throughout the concrete mixture. The mixture consistency for SRW blocks is achieved by reducing the amount of water or by lowering the paste fraction of the mixture [24]. The cement paste is usually more heterogeneous and the water dispersion is much more uneven than conventional concrete mixtures.

2.4.1 SRW Block Pore System

The structure of SRW blocks contain aggregate and paste, along with larger pores referred to as compaction voids that can be as large as 2 to 3 mm (0.08 or 0.10 in). The size of these voids is directly related to the distribution of the aggregates in the mixture

and the energy of compaction during production [25]. Figure 2.3 shows typical compaction voids and air voids found in SRW blocks.

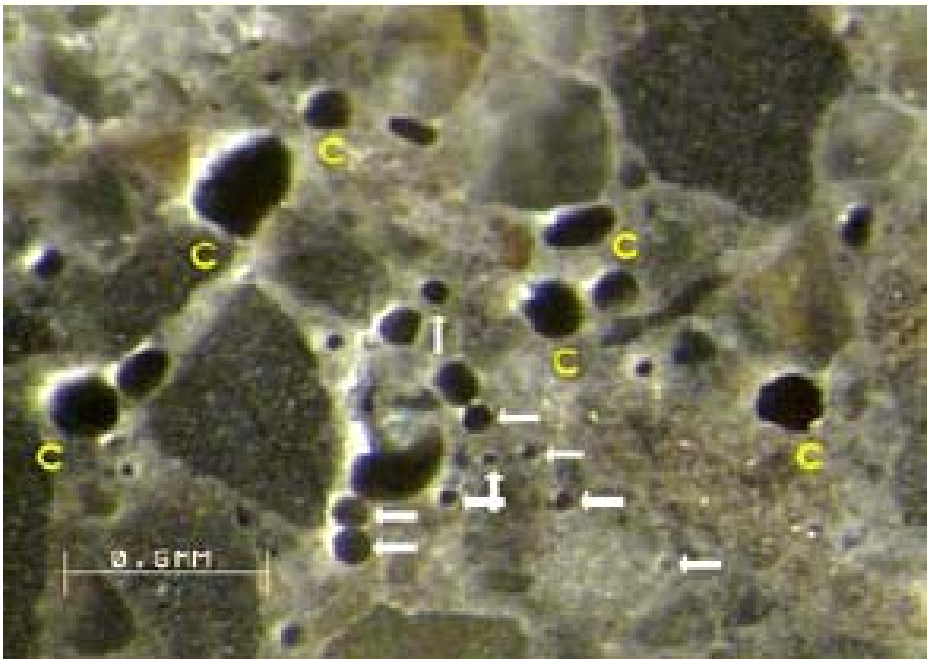

Figure 2.3 SRW block displaying typical air (arrow) and compaction voids (C) [25].

The correlation between freeze-thaw resistance and compaction voids in SRW blocks is not well understood. Some research has indicated that small and isolated compaction voids can act as efficient escape boundaries and provide protection against freeze-thaw deterioration [26]. A contrary theory states that the compaction voids do not aid in protection against frost damage because it is believed that these large voids contribute to the fast saturation of the cement paste [27]. Saturation of the paste is thought to allow freeze-thaw damage to occur rapidly.

Another difference in the SRW block microstructure from that of traditional concrete is the highly porous paste-aggregate interface. In SRW blocks, the paste-aggregate interface is less dense than the rest of the paste and contains initial

microcracks. This highly porous interface is thought to be caused by the high degree of stiffness of the dry mixture, were the paste is restricted from moving around the aggregate particles during mixing. Further research is needed to completely understand the cause of the less dense paste-aggregate interface found in SRW blocks.

A petrographic analysis performed by MacDonald et al. on thin sections cut from SRW blocks found that both compaction voids and air voids were present in a typical SRW block microstructure [28]. The compaction voids were randomly oriented and were irregularly shaped, while the other air voids were typically smaller in size and spherical in shape. There was no correlation found between the air void structure and the freeze-thaw durability.

A year later, MacDonald and Lukkania [29] revisited the study concerning the influence of the microstructure on freeze-thaw resistance. In this study, they investigated the void systems more in depth, exploring the void systems with respect to the capillary voids and gel pore systems, along with compaction voids. The researchers identified the importance of proper curing techniques that result in a better defined pore system. It was found that a proper curing regime can reduce the amount of available free water for freezing and provide better freeze-thaw resistance regardless of the characteristics of the compaction porosity [29].

An air void analysis of SRW blocks was also conducted by Haisler et al. [3]. They noticed significant differences between SHA approved and non-SHA approved SRW blocks. An extensive network of compaction voids was identified for both block types. It was observed that only a portion of the compaction voids were bound by hydrated cement paste for the non-SHA approved blocks. The SHA approved blocks consisted of much higher paste contents and displayed more homogenous internal structures. Samples were tested according to the standard ASTM C 1262, *Standard Test Method for Evaluating the Freeze-Thaw Durability of Manufactured Concrete Masonry Units and Related Concrete Units* [4]. The study indicated there was a good correlation between air void content and freeze-thaw durability [3]. Samples with an air void content less than 16 percent were the least durable. An indicator of freeze-thaw durability was found to be the ratio of specific surface area to the total volume of the voids. Samples

with a ratio below 1mm^2/mm^3 (0.04 in^2/in^3) were able to exceed 50 freeze-thaw cycles in water or 25 freeze-thaw cycles in 3 percent NaCl solution. Samples with a value greater than 1mm^2/mm^3 (0.04 in^2/in^3) all lasted over 100 cycles. Overall, the researchers concluded that the internal structure of the blocks had a significant impact on the performance of the units when subjected to freeze-thaw cycles.

2.4.2 Air Entrainment in SRW Blocks

As noted earlier, air entrainment in conventional concretes contributes to protection against freeze-thaw damage. The hydrated cement paste in typical concrete accounts for approximately twenty-five percent of the entire concrete volume. This quantity of paste allows for the even distribution of entrained air voids. However, unlike conventional concrete, SRW blocks contain limited amounts of hydrated cement paste. Also, these blocks are fabricated using very dry mixtures. These dry mixtures require intense compaction during fabrication and this compaction can result in the coagulation of the entrapped air voids.

Problems occur with the use of air-entraining agents in the manufacturing of dry cast SRW blocks because the production method used to fabricate these blocks and the resulting microstructure make it difficult for the entrained air to be dispersed throughout the cement paste. The microstructure of SRW blocks is much more heterogeneous than typical concrete because the cement paste is generally not evenly dispersed throughout the mixture. Without complete spreading of the cement paste, the entrained air can not be evenly distributed. Air voids must be closely spaced and evenly distributed, separated by a distance of 0.1 to 0.2 mm (0.004 to 0.008 in), for potential escape boundaries used by freezing water.

Hazrati and Kerkar [25] studied the affect of an air-entraining admixture in dry cast masonry products on freeze-thaw durability. They developed and patented an admixture (US patent 6,258,161 and 6,302,955) that entrained air, up to 3 percent by volume, in the SRW blocks. The researchers tested samples according to the ASTM C 1262 standard test method to assess the freeze-thaw durability of different mixture designs [4]. They found that the freeze-thaw durability increased by 95 percent for

mixture proportions containing the air-entraining admixture. Also, the admixture helped to disperse the cement paste, which increased the degree of hydration and produced an ample amount of escape boundaries, all of which increased the freeze-thaw durability. However, other research has found that air entrainment in SRW blocks has not been effective.

2.5 RESEARCH ON FREEZE-THAW DURABILITY FOR SRW BLOCKS

Compared to conventional concrete there has been limited research on the freeze-thaw durability for SRW blocks. However, some research has been performed to investigate parameters that are thought to influence freeze-thaw durability. Also, some field studies have been completed in an attempt to better understand the origin of SRW blocks that failed due to freeze-thaw exposure.

2.5.1 Laboratory Based Freeze-Thaw Tests on SRW Blocks

Bremner and Ries used the ASTM C1262 standard test method to examine the freeze-thaw resistance of normal weight and lightweight concrete mixes [4,30]. The results indicated that only a slight difference in resistance exists between the two concrete types. However, the experiment found that as the compression strength increased, the freeze-thaw resistance also increased. Bowser et al. completed a series of experiments using the ASTM C 666 standard test method to test SRW blocks [31,20]. These researchers also tested normal and lightweight concrete mixtures that included silica fume, fly ash, and/or other admixtures. The experiments concluded that the durability of the lightweight concrete was better even though the absorption was higher for these concretes or blocks. There was evidence that the normal weight concretes or blocks containing pozzolans had less resistance to freeze-thaw damage. It was also noted that SRW blocks containing a waterproofing admixture resulted in high freeze-thaw durability and low absorption rates for the lightweight mixtures.

Two studies were conducted by the National Concrete Masonry Association (NCMA) to assess the freeze-thaw resistance of concrete masonry units including SRW blocks. The first of the two tests indicated that the freeze-thaw resistance for SRW

blocks increased as the density and compression strength increased, but decreased as absorption increased [32]. They also found that samples exposed to a 3 percent NaCl solution experienced failure 10 to 20 percent sooner than those exposed to fresh water. The second study varied the mixture proportion to assess their performance to freeze-thaw conditions [33]. The study resulted in an increase in resistance as the cement content was increased and an increase in freeze-thaw resistance as the admixture's contents were increased. Again, the SRW blocks exposed to the 3 percent saline solution experienced early failure, and none of the blocks exceeded 50 freeze-thaw cycles.

An experiment completed by Scott evaluated SRW blocks from different manufacturers throughout the United States and Canada [34]. The blocks had different aggregate types and cement contents. The SRW blocks also varied in absorption and compression strength. The ASTM C 1262 test was used to evaluate the samples [4]. In this study, absorption characteristics and aggregate types were found to be insignificant factors influencing the freeze-thaw durability. The compression strength of the samples was positively correlated with the durability of the SRW blocks. The experiment also revealed that the least durable block had more than 15 percent air content, while the more durable had less than 9 percent.

2.5.2 Field Evaluations of SRW Block Freeze-Thaw Durability

Several field studies were conducted in the northeastern United States where freeze-thaw conditions are prevalent. The field evaluations produced results similar to laboratory experiments pertaining to the importance of freeze-thaw durability research on SRW blocks.

Embacher et al. conducted an extensive field evaluation of SRW block freeze-thaw durability along roadways [1]. The objective of the field evaluation was to investigate the premature deterioration of SRWs in the area of St. Paul and Minneapolis, Minnesota. The study was performed to determine the proportion of the blocks in areas showing visible signs of distress, and then assess the types and severity of the distress, and finally to identify the factors that might be causing the damage to the walls.

The examination included walls that were constructed during or before 1994, walls built at the same time but face opposite directions, and a few privately owned walls that were subject to failure. Information on wall location, environmental conditions, the design/construction method, concrete block specifications, and maintenance records were recorded for each wall. The investigator assigned each wall with a distress rating from 0 to 5, with the highest value having no visible distress and the lowest value showing high levels of distress.

After compiling these data, Embacher found that only 7 percent of the walls surveyed showed significant deterioration. But 50 percent of the walls revealed signs of freeze-thaw damage, spalling, scaling, embedded vegetation growth, manufacturing flaws, efflorescence, wash-through, and open joints. A substantial amount of the walls inspected exhibited freeze-thaw damage. This freeze-thaw damage occurred in areas of the blocks where saturation was the greatest. The freeze-thaw damage seemed to be dependent on the wall age and block manufacturer. The cause of this damage was thought to be a result of improper mixture designs, nondurable aggregates, and inadequate curing procedures. Embacher recommended that manufacturers make the blocks more durable, test blocks to identify durability mechanisms, implement evaluations of field exposure sites, and to develop test methods that better represent actual field conditions.

Another field study was conducted by Haisler et al. while visiting several SRWs throughout Wisconsin and Minnesota in August of 2003 [3]. The research team located and photographed existing walls to document their level of damage. They also obtained limited samples from the walls for laboratory testing. Fourteen walls were examined in Wisconsin and Minnesota. Five walls in Wisconsin and seven walls in Minnesota showed significant freeze-thaw damage. However, these walls were chosen because damage was previously known to exist. The team identified two main types of freeze-thaw indicators: salt scaling of the exposed face and internal microcracking. It was observed that deterioration of a block occurred due to a combination of both cracking and scaling [3]. These two mechanisms of damage can lead to the replacement of particular

blocks or an entire wall. Figure 2.4 illustrates how SRW blocks typically crack because of hydraulic pore pressures due to freezing water.

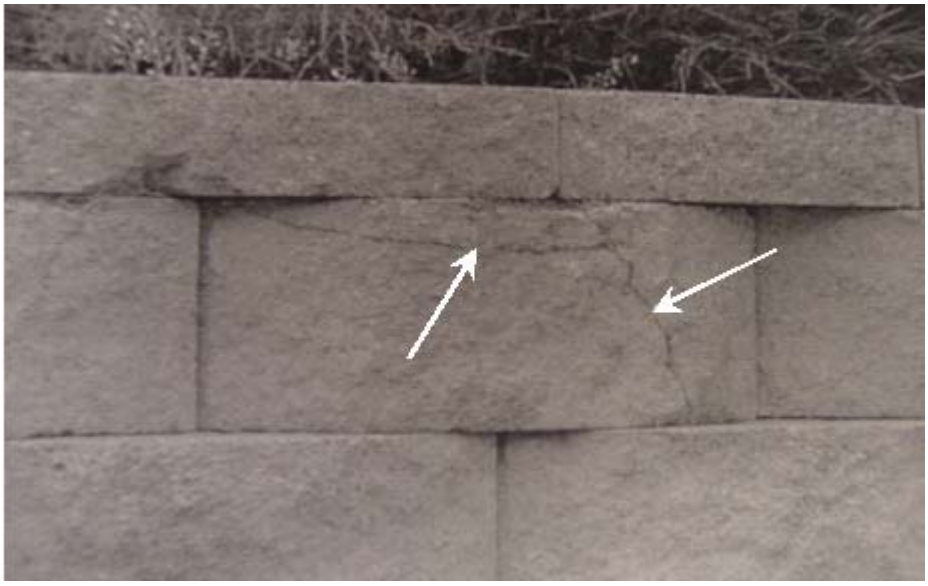

Figure 2.4 Cracks on SRW block facing due to freeze-thaw microcrack propagation [3].

Haisler et al. also studied the variables that affect the field performance of the SRWs [3]. The main variables evaluated include: exposure conditions, the type of block used, and construction techniques used when constructing the wall. Walls located in areas with poor drainage, such as those located in direct drainage paths from roadways or parking lots, exhibited the most damage. Also, the presence of chemicals and salts in the water drained from these areas was thought to be a major factor in damage.

Another prevailing environmental condition that showed extensive damage was areas along roadways where the SRW blocks were exposed to salt spray. Significant damage was evident on blocks at the lower portions of the walls where salt accumulated by the piling of snow and salt against the wall, or where blocks were exposed to salt

spray from passing vehicles [3]. The walls that were exposed to poor drainage exhibited more severe damage than those only exposed to salt spray.

The type of SRW block and the construction technique used also played a key role in their susceptibility to freeze-thaw damage. The types of blocks found in the walls were solid-formed rectangular blocks and split-faced modular blocks. Whether or not more damage on the solid-formed rectangular blocks or the split-faced modular blocks was evident was not discussed.

Construction techniques included wall blocks that were placed directly above and below the other blocks and staggered blocks that allowed for a portion of the top face to be exposed to moisture. The walls constructed with a staggered design exhibited more freeze-thaw damage than those that were stacked directly on top of each other. The ledges formed by the staggered design allowed for an accumulation of moisture and salt to form and led to more damage. Some of the walls with the SRW blocks stacked directly on top of each other had some damage, but not as extensive as the staggered construction.

The research group obtained several field samples that showed evidence of freeze-thaw damage [4]. The samples were evaluated with ASTM C 1262, chloride penetration testing, and microstructural analysis [4]. The samples subjected to the freeze-thaw test method had 100 percent mass loss before reaching 100 freeze-thaw cycles. The chloride profiling tests resulted in a high percentage of chloride ions present on the front face of the blocks, which indicated substantial chloride ion exposure. All samples had large compaction voids and low paste contents, which, as already noted, tends to result in poor freeze-thaw durability.

3. TEST MATERIALS, METHODOLOGIES, AND EXPERIMENTAL DESIGN

3.1 FREEZE-THAW TEST SETUP

One of the tasks of this research is to develop a preliminary test method that provides more realistic testing and performance information for SRW blocks exposed to freeze-thaw conditions. It is apparent that the test conditions should mimic as much as possible real-life freeze-thaw environmental conditions while at the same time being practical for laboratory testing. These environmental conditions should include freeze-thaw cycling and exposure to deicing solutions containing chloride ions as these parameters can significantly influence the performance of SRW blocks.

Some important equipment necessary for developing the test setup are programmable environmentally controlled facilities, a spray system with cyclic capabilities, and a test chamber large enough to hold six to nine SRW blocks. The environmentally controlled facility should be capable of controlling the temperature from -20°C to 24°C (-4°F to 75°F). The environmental facility should have heating and cooling capabilities of at least 0.55°C (1°F) per minute. The programmable temperature controller for the environmental facility should allow the researchers to set the desired temperature ramping rates, hold times, and number of freeze-thaw cycles to be repeated. A typical environmental room temperature cycle is shown in Figure 3.1.

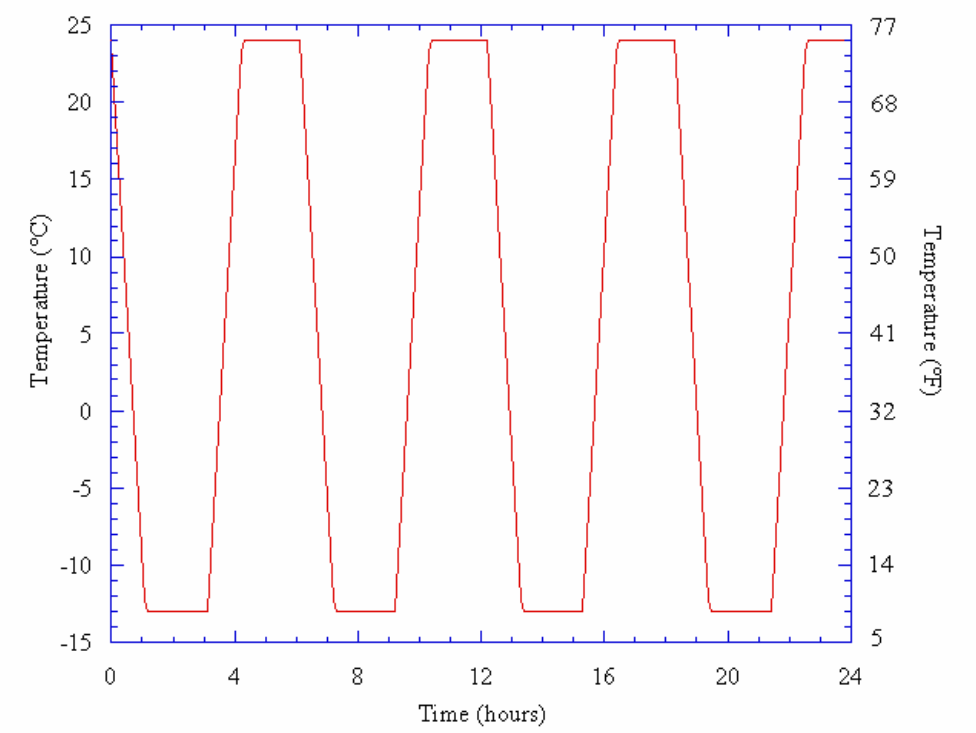

Figure 3.1 Typical environmental chamber temperature cycle.

The chamber that houses the SRW blocks should incorporate a spray system for applying chloride containing or fresh water solutions. For this research, the test setup was designed to withstand the harsh freeze-thaw and chloride conditions, while being durable and relatively inexpensive to construct. A detailed drawing of the exposure chamber used in this study is shown in Figure 3.2.

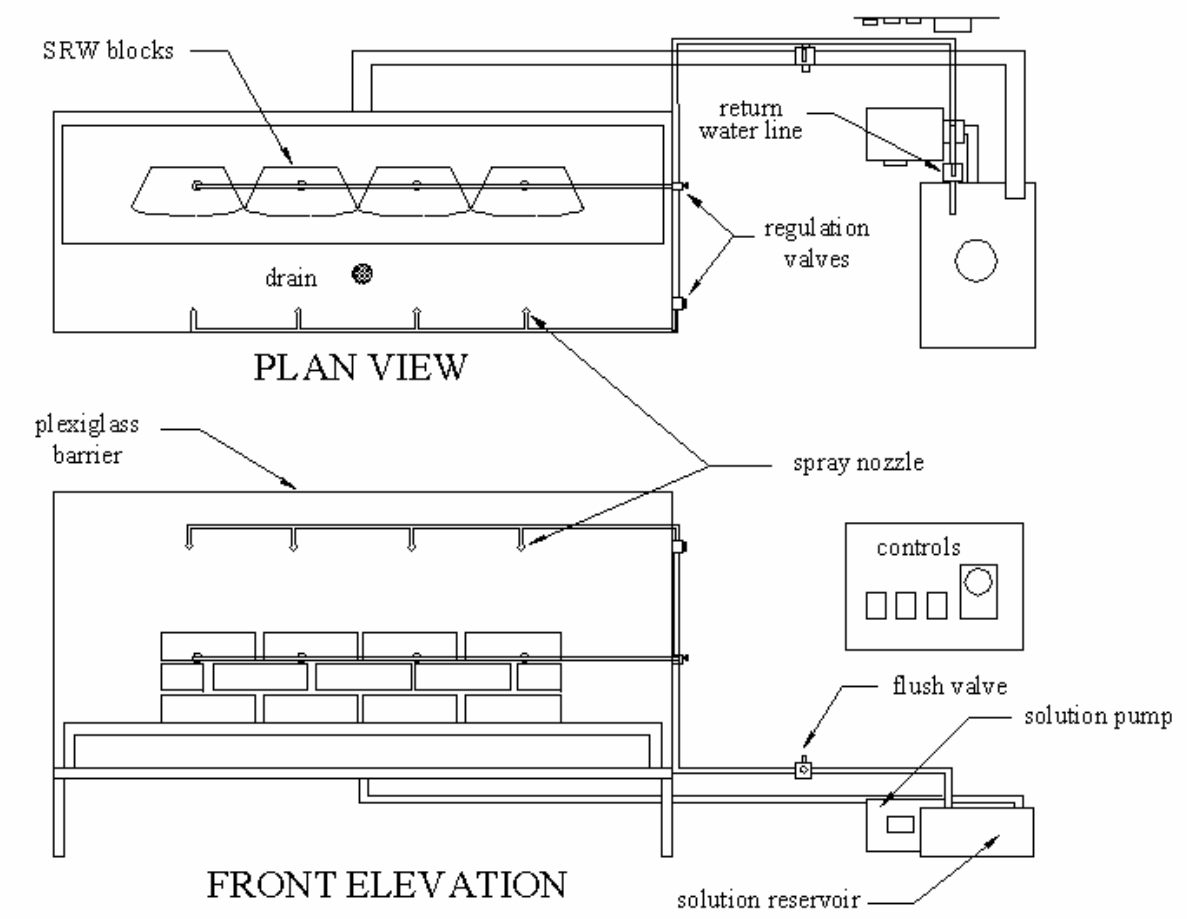

Figure 3.2 Exposure chamber drawing.

The overall dimensions of the chamber were 0.9 m wide, 1.8 m long, and 1.5 m tall (3 ft by 6 ft by 5ft). The chamber support structure was built with a 51 mm (2 in) angle iron frame to support the weight of the SRW blocks. The sides of the chamber were fixed with sheets of plexi-glass to retain the spray solution during testing. The bottom drain section of the test system was be constructed with a decreasing slope toward the center to ensure complete drainage of the solutions. A 25 mm (1 in) steel angle was also welded around the top edge of the frame so the bottom of the plexi-glass barrier would fit within the frame to contain the solution within the chamber. The structure was bolted together so that it could be easily assembled and disassembled inside the

environmental room. The entire structure was painted with an industrial enamel to prevent corrosion. It should be noted that alternate designs with similar conditions may be feasible for testing SRW blocks

The spray system consists of eight 6 mm (0.25 in) stainless steel spray nozzles with 2 mm (0.081 in) maximum free passage orifices and a 19 L (5 gal) per minute maximum flow rate to ensure complete coverage of the SRW block samples. The spray nozzles were attached to 9.5 mm (0.375 in) stainless steel tubing that was fixed in the chamber. Four nozzles were positioned in front of the wall and four above the wall to ensure complete exposure to the de-icing solution or fresh water. Also, a ball valve was placed before each set of nozzles to regulate the flow from the front or top nozzles to the SRW blocks. The spray system was supplied with a PVC water pipe connected to a ¾ HP 316 stainless steel centrifugal pump rated for pumping the 3 percent NaCl to withstand the corrosion susceptible conditions.

The solution pump can be controlled by electrical or mechanical timers that enable the pumps to turn on for a fifteen minute interval when the environmental room is thawed. The required solution is pumped from a 49 L (13 gal) polypropylene reservoir. There is a return line from the discharge of the pump to regulate the back pressure that could cause damage to the pump. Back pressure could exist if the spray nozzles become blocked.

The drain system on the test setup had a 31.75 mm (1.25 in) PVC gravity flow drain line from three 50.8 mm (2 in) PVC drains in the bottom of the floor back to the solution reservoir so that the pumped solution can return to the reservoir quickly. All of the PVC piping in the exposed freezing conditions was insulated with foam pipe insulation to protect the pipes from cracking under freezing conditions.

A photograph of the test setup is shown in Figure 3.3. The plumbing, solution pumps, and reservoirs are separated from the test chamber by an insulated wall to protect the pumps and plumbing from freezing temperatures. There is also a halogen heat lamp in this area to keep the equipment warm and to provide light to work.

Figure 3.3 Front view of test chamber.

3.2 PROOF OF CONCEPT TEST

A preliminary freeze-thaw test procedure was developed and used to assess the freeze-thaw performance of SRW blocks to provide preliminary information on the test procedure. The proof of concept test was performed to identify and repair any problems with the initial setup, identify key parameters of the experiment, and set standards for the procedure. The focus of developing this new test method was to replicate field environmental conditions as closely as practical by implementing slower temperature changing rates, longer temperature hold times, and spray exposure conditions instead of ponding. It is anticipated that environmental conditions similar to those found in the field will provide modes of the SRW blocks that reflect those observed in the field. It is essential that this process provide information on the freeze-thaw durability of the blocks while at the same time providing a simplistic and timely test procedure. It is hoped that

ultimately, this test method will offer manufacturers and SHAs important field freeze-thaw performance and life-cycle information.

3.2.1 Proof of Concept Test Materials

For the proof of concept test standard commercial landscaping SRW blocks were purchased at a home supply store. The typical dry weight of the commercially available SRW block was 12 kg (26.5 lbs) and the dimensions of these blocks are shown in Figure 3.4. All of the surfaces were smooth except the front split face that had a rough texture (aesthetically more desirable).

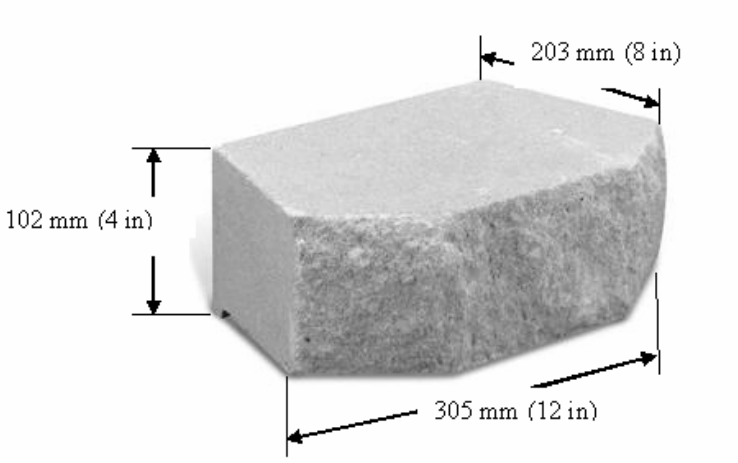

Figure 3.4 Commercially available SRW block.

3.2.2 Diffusion Coefficient Determination for Small Commercial SRW Blocks

Because these blocks would be used for the preliminary freeze-thaw test it was essential to determine the apparent diffusion coefficient for the block material to determine the rate that the chloride ions are transported into the SRW blocks. This information could provide researchers information on how the material is affected by the chloride ions and the use of this information can then be used to estimate freeze-thaw

durability. Blocks were procured and cut into four sections. For characterization of the diffusion coefficient, each of the sections was coated with a low viscosity epoxy coating, leaving only the front textured surface exposed. Small plexi-glass dams were placed around the exposed front and the interface of the block and dams were sealed again with an epoxy. Three samples were randomly selected from each block and the reservoirs were filled with a 3 percent NaCl solution. Ponding was continuous. The NaCl was removed from the dams after various exposure times to determine chloride diffusion coefficients. Diffusion coefficients were determined after one, three, and six weeks of exposure following a modified version of *The Standard Test Method for Total Chloride Content in Concrete Using the Specific Ion Probe* [35]. The specific ion electrode was calibrated using standard concentrations of NaCl calibration solutions. Readings were taken for each calibration solution and a regression was performed prior to testing to determine characteristic constants used in diffusion coefficient calculations.

Mortar samples from the profile grindings were taken at three millimeter intervals. This provided 1.5 ± 0.1 g (0.5 ± 0.004 oz) of material for testing. The material was weighed and placed in clean plastic bottles. The required solutions, a digestion solution (acetic acid, isopropyl alcohol, and distilled water) and a stabilizing solution (3.75 ppm NaCl solution), for the test method was mixed with the mortar powder and a voltage reading was taken using the specific ion probe for each sample. Calculations were performed to determine the percent chloride at various depths for each of the samples as follows:

$$\%Cl^{-} = (10.00^{(C+D\cdot M)} - 3.00 \cdot 0.00333) \tag{3.1}$$

where C and D are the characteristic constants of the electrode calibration curve (y = C + Dx) and the term M is the specific ion probe reading in millivolts.

The percent chloride concentration data collected provides an indication on the rate at which the chloride ions are transported into the SRW blocks over time. The fresh unit weight of the SRW block material is traditionally used in the test procedure to

calculate the actual content of chlorides in kilograms per cubic meter (pounds per cubic yard) of material. However, this information was not known for the SRW blocks because they were cast at a production plant. As a modification to the procedure, the half-saturated unit weight was thought to be a sufficient estimate of the fresh unit weight. To achieve this calculation a small sample of block was cut and submerged in distilled water and weighed every 24 hours until the percent mass gain was negligible. The mean value between the dry and saturated masses along with the volume of the sample was evaluated to determine the unit weight. This average was used in the calculation because SRW blocks are formed using a dry concrete mixture. It was believed that a fully saturated mass would over estimate the fresh unit weight. The SRW blocks were determined to have a saturated unit weight of 2146 kg/m^3 (3647 lb/yd^3). The equation used to determine the chloride content in kilograms per cubic meter of SRW block cementitious material is shown below:

$$Cl^{-}(kg/m^3) = 0.5937 \cdot (10.00^{(C+D \cdot M)} - 3.00) \cdot 0.00333 \cdot W \cdot 10^{-2} \tag{3.2}$$

where W is the saturated unit weight of the SRW block in kg/m^3. After the concentrations of chloride ions in the samples were calculated the apparent diffusion coefficients were determined by fitting a curve to the chloride concentration versus the depth of the chloride using the following equation:

$$C(x,t) = C_0 \cdot erfc\left(\frac{x}{\sqrt{4 \cdot D_a \cdot t}}\right) \tag{3.3}$$

where C_0 is the chloride concentration at the surface of the block sample in kg/m^3, x is the mean depth of the dust sample in meters, t is the time in seconds that the chloride was exposed to the SRW block, and D_a is the diffusion coefficient in m^2/s. The Goal Seek function in spreadsheet programs can be used to find appropriate diffusion coefficient

values. The mean value of the different depths is then reported as the diffusion coefficient for each sample.

3.2.3 Chloride Diffusion Coefficient Results from Small, Commercial SRW Blocks

The chloride transport data were collected and the diffusion coefficient calculations were completed for the commercially available SRW landscaping blocks. After the chloride concentration was measured for each sample a curve was generated. The results for each block sample are shown in Table 3.1. The chloride threshold curves for each exposure time are shown in Figure 3.5.

Table 3.1 Diffusion coefficient results.

Sample	*Exposure Time*		
	1 Week	*3 Weeks*	*6 Weeks*
1	2.96E-10 m^2/s (4.59E-7 in^2/s)	4.10E-11 m^2/s (6.36E-8 in^2/s)	3.67E-11 m^2/s (5.69E-8 in^2/s)
2	6.90E-11 m^2/s (1.07E-7 in^2/s)	5.92E-11 m^2/s (9.18E-8 in^2/s)	1.59E-10 m^2/s (2.46E-7 in^2/s)
3	1.54E-10 m^2/s (2.39E-7 in^2/s)	5.89E-11 m^2/s (9.13E-8 in^2/s)	3.70E-11 m^2/s (5.74E-8 in^2/s)
Mean	1.73E-10 m^2/s (2.68E-7 in^2/s)	5.30E-11 m^2/s (8.22E-8 in^2/s)	7.76E-11 m^2/s (1.20E-8 in^2/s)
Std. Dev.	1.15E-10 m^2/s (1.78E-7 in^2/s)	1.04E-11 m^2/s (1.61E-8 in^2/s)	7.05E-11 m^2/s (1.09E-8 in^2/s)

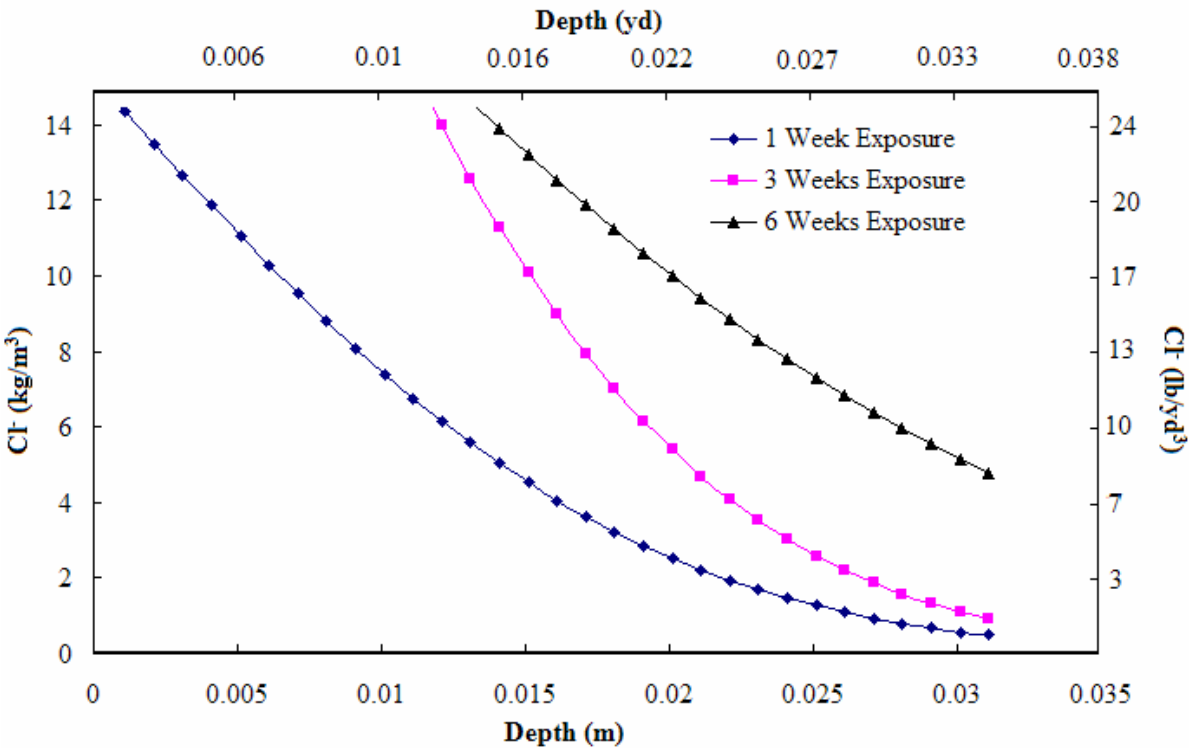

Figure 3.5 Chloride ion concentration curve for block samples.

Note that one sample from each block was exposed to NaCl for each of the specified periods. Overall, the apparent chloride diffusion coefficient values tended to decrease, and the chloride threshold curves tend to shift upward as the exposure time increases. The chloride diffusion coefficient of conventional cast-in-place concrete is typically one or two orders of magnitude smaller than those found for the SRW blocks. These results indicate that the SRW blocks have much more interconnected pores than conventional concrete, allowing chloride ions to be transported throughout the material faster.

3.2.4 Proof of Concept Freeze-Thaw Test Setup and Variables

Four experiments were completed during the proof of concept test. Table 3.2 provides an overview of the parameters investigated for each of the tests.

Table 3.2 Proof of concept experimental design.

Commercially Available Landscaping SRW Blocks		**Temperature Hold Time (hours)**	**Percent NaCl**	
			0	3
Environmental Room Temperature Ramping Rate °C/min (°F/min)	0.18 (0.3)	1	*No Test*	*Test 2*
	0.33 (0.6)	1	*Test 3*	*Test 4*
	0.55 (1.0)	2	*No Test*	*Test 1*

The preliminary proof of concept testing consisted of testing sets of thirteen SRW blocks. To prepare the blocks for testing, the blocks were oven dried at 113°C (235°F) for twenty-four hours, then marked for identification and weighed. After the block weights were recorded, the blocks were submerged in water. The blocks were then removed from the submerged condition, surface dried, and weighed every 24 hours to ensure saturation. The blocks became fully saturated after approximately 48 hours of submersion.

The blocks were then stacked in the freeze-thaw chamber as shown in Figure 3.6. The first three rows of blocks labeled A through L were used for mass loss measurements. The top block, indicated as M, was designated for temperature measurements.

Figure 3.6 Freeze thaw setup of SRW blocks.

To evaluate the internal temperature of the SRW blocks a 6.35 mm (0.25 in) hole was drilled in the back of block M to the center of the block. A Type J thermocouple was then inserted into this hole and the hole was backfilled with approximately 25.4 mm (1 in) of mortar made from a mixture of water, cement, and the block drill dust. The remaining hole was then filled with an insulating foam spray. The block temperature ramp rates and hold times were monitored to define the appropriate parameters for the actual test. The center of the block temperature decreased at a rate of approximately 0.12°C (0.30°F) per minute and during the thaw cycle the temperature increased at a rate of approximately 0.06°C (0.10°F) per minute. Figure 3.7 shows the temperature ramping rates of the center of the SRW block compared to the environmental room temperature.

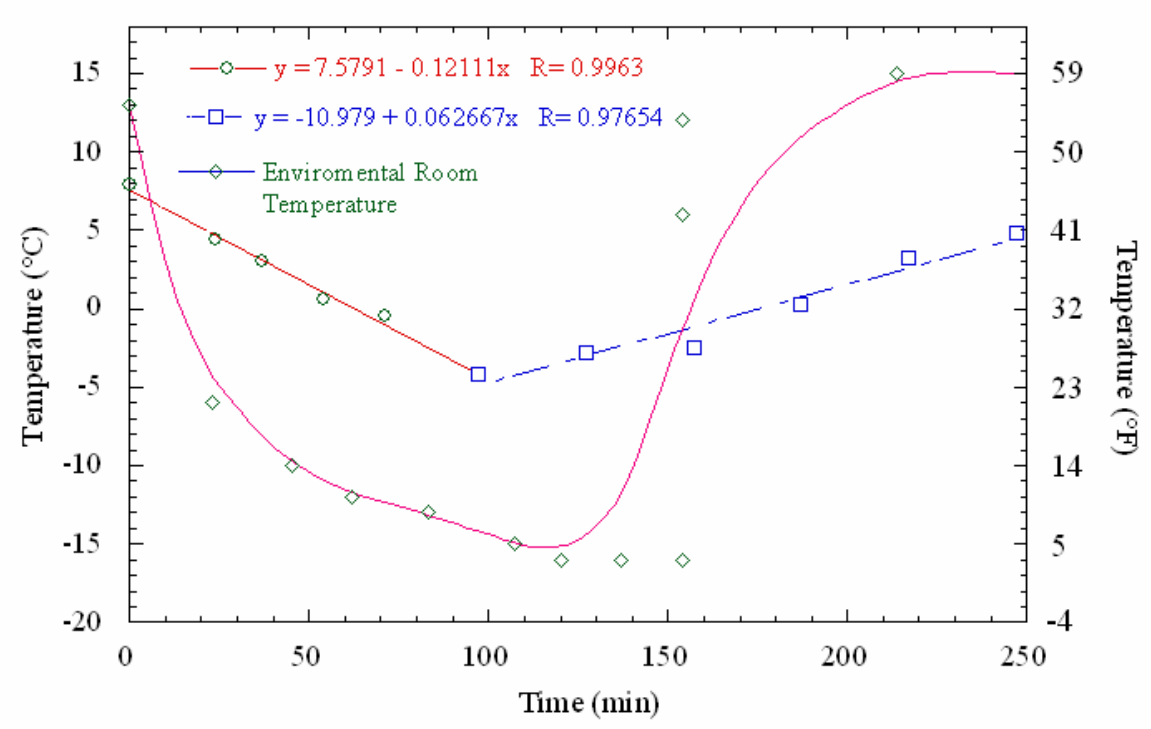

Figure 3.7 SRW block temperature changing rates.

3.2.5 Proof of Concept Freeze-Thaw Test Procedure

The blocks were subjected to two freeze-thaw cycles per day. The first test was done by manually changing the temperature setting for the environmental room from -18°C to 16°C (0°F to 60°F), which produced block temperature ramping rates shown in Figure 3.7 and environmental room ramping rates of 0.55°C (1°F) per minute. The cycles consisted of thawing for three hours and then freezing for three hours with a one hour ramp time and a two hour hold time. The blocks were subjected to freezing temperatures over night and thawing began the following morning. The blocks were sprayed with NaCl for 15 minutes prior to the freezing cycle. The samples were exposed to 10 freeze-thaw cycles and then evaluated for freeze-thaw damage by visual inspection. These blocks were then saturated for twelve hours to restore any evaporated moisture during the testing. After weighing, they were restacked in the chamber in the same order as the original stacking. Photographs of the blocks were obtained for a visual record and the test cycle was repeated. When all of the blocks reached an Embacher Severity Level, as explained in section 3.3.5 of this report, of high the system was considered to have failed.

Shortly after the first experiment was completed, the programmable controller was installed and used to automatically change the temperature in the room. The controller enabled temperature changing rates of 0.18°C (0.3°F) and 0.33°C (0.6°F) per minute. Tests were completed for each of these environmental room ramping rates with an exposure of 3 percent NaCl solution. An additional test with an environmental room ramping rate of 0.33°C (0.6°F) per minute and an exposure to fresh water was also completed. An overview of the test procedure for the proof of concept test is shown in Figure 3.8.

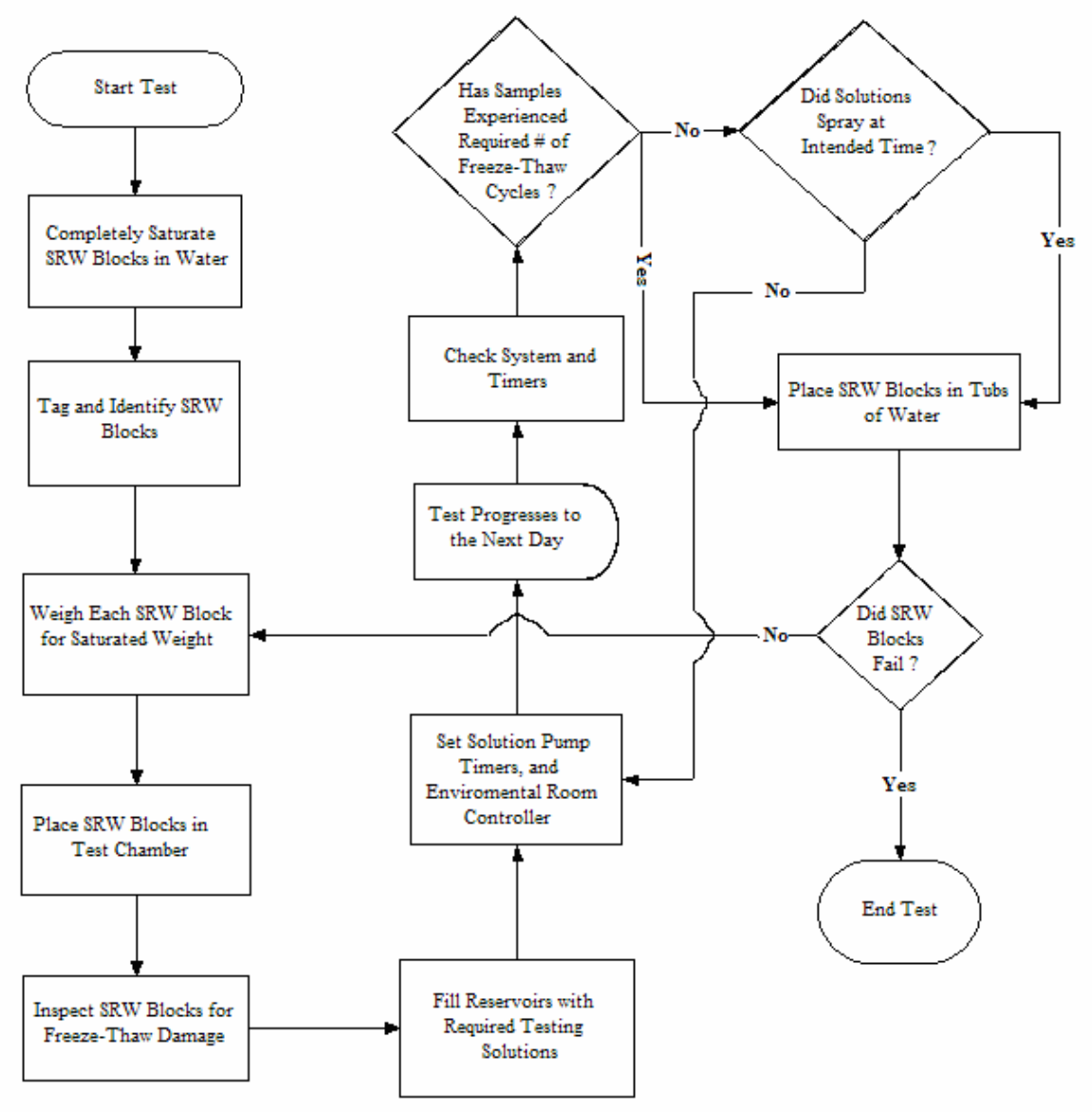

Figure 3.8 Proof of concept test procedure flow chart.

3.2.6 Proof of Concept Freeze-Thaw Mass Loss Results

During the first test (identified as Test 1), the SRW blocks were thawed and taken out of the chamber after ten freeze-thaw cycles. The blocks were then immersed in water overnight to regain any lost moisture and to rinse off any debris. The surfaces of the samples were towel dried and the block samples were weighed. The percent mass loss

was calculated after every ten cycles to assess the deterioration of the SRW blocks. A sample calculation for assessing percent mass loss is as follows:

$$\%\,Mass\,Loss = \left(\frac{(mass_{\,2} - mass_{\,1})}{(mass_{\,1})} \right) 100 \qquad (3.4)$$

where $mass_2$ = the mass of the sample after the 20 freeze-thaw cycles and $mass_1$ = the mass of the sample at the beginning of the test.

The majority of the blocks experienced a mass gain over the first twenty cycles. This could be due to the expansion of the pore structures within the blocks allowing more water to be absorbed. However, the weight gain decreased as more freeze-thaw cycles were performed. After thirty cycles the blocks began to loose their integrity and the mass loss increased substantially. A graph showing the trend of mass loss during Test 1 for each of the blocks can be seen in Figure 3.9.

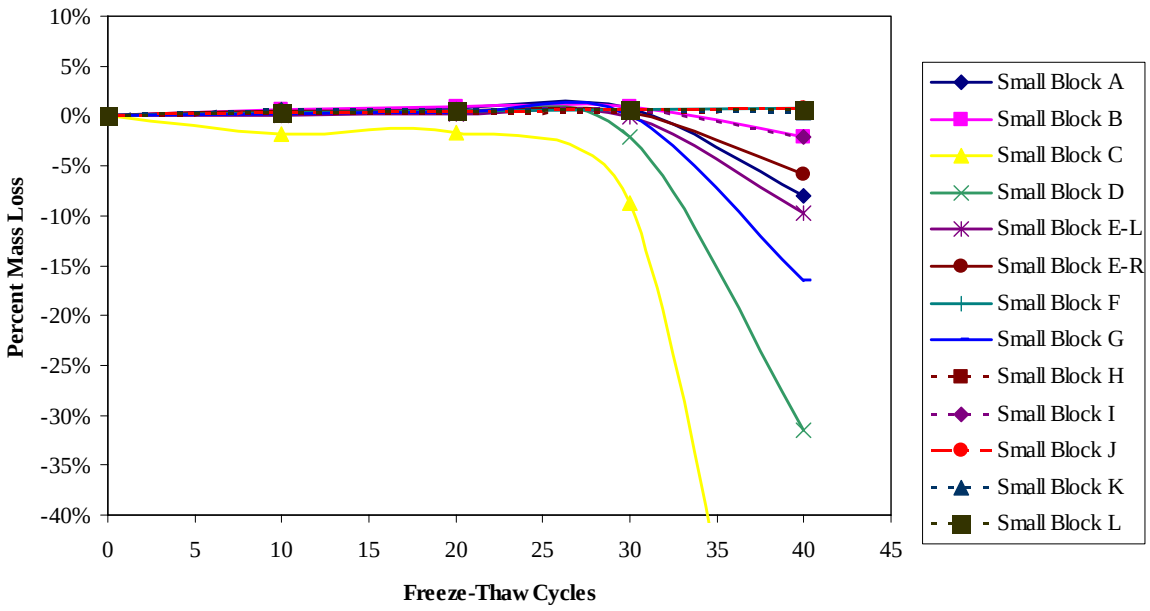

Figure 3.9 Percent mass losses from Test 1.

Figure 3.9 shows that many of the blocks began to exhibit mass loss after approximately twenty or thirty freeze-thaw cycles. Blocks C and D exhibited significant freeze-thaw damage and deteriorated rapidly. The test was continued until damage was evident on each of the blocks. The damage assessed on the SRW blocks replicated the same modes of failure (cracking and salt scaling) as was shown in the field studies identified in the literature review.

An additional experiment implementing an environmental room ramping rate of 0.18°C (0.3°F) was completed (identified as Test 2). This low ramping rate was chosen because it was more representative of field exposure conditions. It was expected that the deterioration speed would be slower so the samples were evaluated after every twenty freeze-thaw cycles. The rest of the test parameters remained the same as the earlier tests. An overview of the results from this test is shown in Figure 3.10.

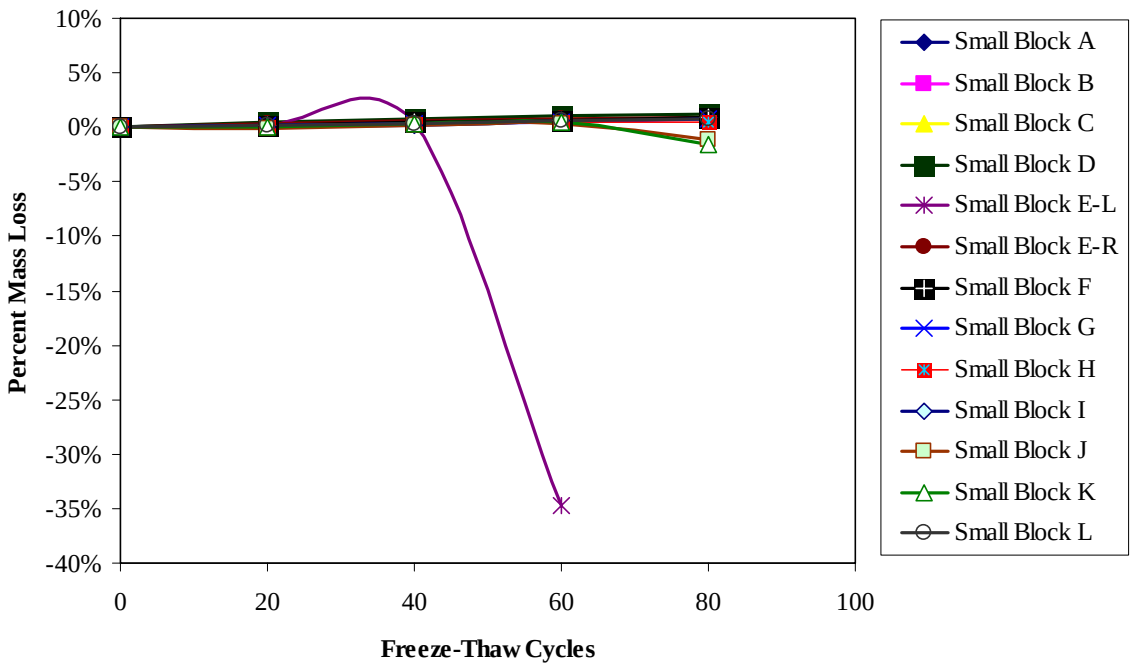

Figure 3.10 Percent mass losses from Test 2.

Blocks A and E-R exhibited substantial deterioration after less than forty freeze-thaw cycles. Block I showed complete failure after sixty cycles and Blocks J and K showed minor failure after eighty cycles. The other blocks had minor freeze-thaw damage at 80 cycles.

Before the next test began, a second test setup was constructed so that two test could be completed at the same time. This experiment consisted of testing two more sets of small commercially available blocks per the defined test procedure. The environmental room ramping rate was set at 0.33°C (0.6°F) for this experiment (referred to a Test 3). One set of twelve SRW blocks was exposed to a 3 percent NaCl solution while the other set of twelve blocks were sprayed with fresh water. The percent mass loss results from SRW blocks exposed to fresh water during thaw cycles is shown in Figure 3.11.

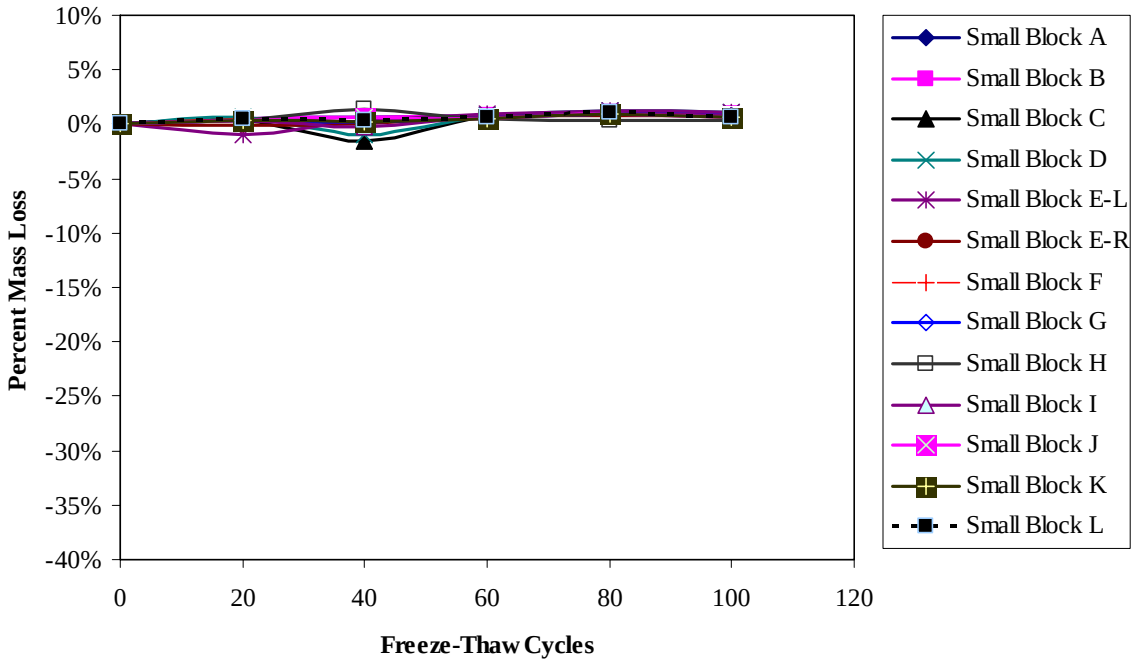

Figure 3.11 Percent mass losses from Test 3.

The results shown in Figure 3.11 of the SRW blocks exposed to fresh water do not indicate any significant freeze-thaw damage. The mass loss values of the blocks tended to fluctuate across a range between two and negative two percent with no noteworthy failures. It was determined that this ramp rate was not desirable for testing due to the longer time required and the good correlation between failure modes of the 0.55°C/min (1°F/min) temperature ramp rate. The results for this experiment where the blocks were sprayed with a 3 percent NaCl solution and exposed to the same ramping rate are shown in Figure 3.12.

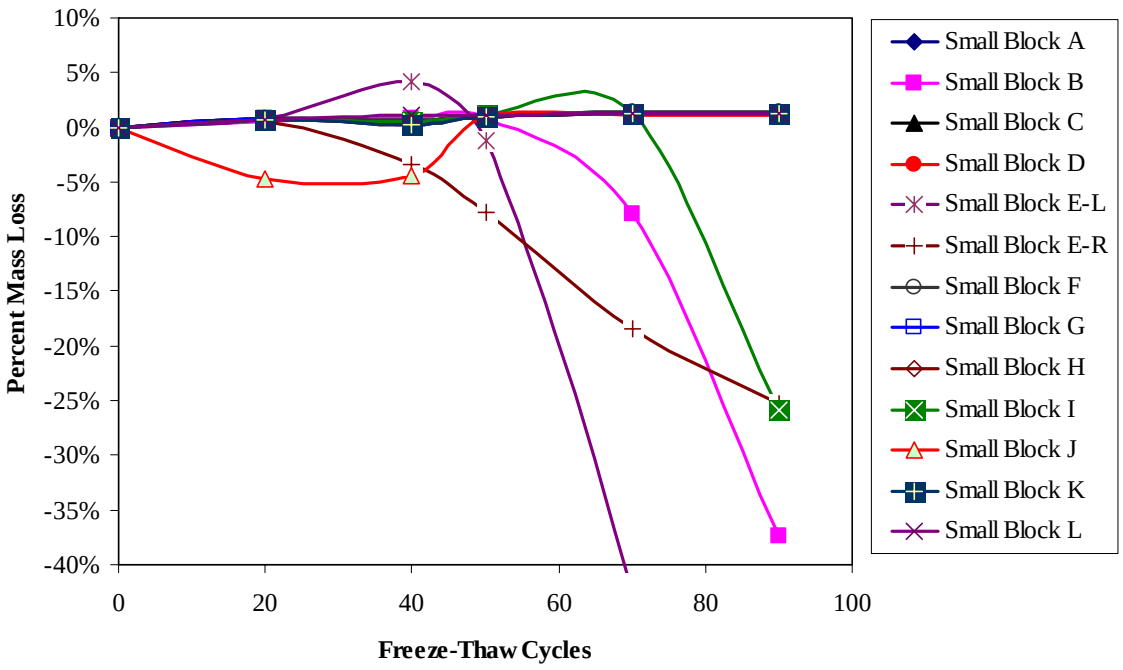

Figure 3.12 Percent mass losses from Test 4.

The results from Figure 3.12 show that four of the blocks exhibited significant damage between forty and eighty freeze-thaw cycles. As before, there was some fluctuation in the percent mass loss for several of the blocks, because of the variation of water absorption of the blocks. Also, notice that two of the samples that failed were

block E-L and block E-R, which were the blocks that were cut in half. This indicates that a cut section of SRW block exposed to a NaCl solution and freeze-thaw conditions is more likely to exhibit damage and early failure. The results from each of the proof of concept tests were similar except for the experiment where the SRW blocks were exposed to fresh water. Results indicate that NaCl exposure is a key factor in damage to the SRW blocks. The different temperature ramp rates did not exhibit a significant difference in the failure rates of the blocks. The first test completed with the most aggressive temperature ramping rate and the longest hold times showed that significant damage occurred on the majority of the blocks in reasonable test periods.

3.2.7 Proof of Concept Freeze-Thaw Visual Inspection Results

Visual inspection results from the first test completed showed significant freeze-thaw damage that closely represented typical degradation of field specimens. Photographs were taken of all of the block faces after every ten cycles to provide evidence of surface degradation. After twenty freeze-thaw cycles, there was some evidence of freeze-thaw damage to several of the blocks. Photos of the typical freeze-thaw damage are shown in Figure 3.13 and Figure 3.14

Figure 3.13a shows freeze thaw damage to the blocks where a corner broke off of the face. Figure 3.13b shows how the faces of the SRW blocks tended to crack and then scale off due to freeze-thaw cycles. Figure 3.14 shows another mode of freeze-thaw damage to the SRW blocks.

(a) ***(b)***

Figure 3.13 Scaling from freeze-thaw damage from Test 1; a) back left corner; b) facial scaling.

Figure 3.14 Typical cracking and spalling from freeze-thaw damage from Test 1.

Figure 3.15 shows how block C further deteriorated after forty freeze-thaw cycles when exposed to saline solutions. A photograph of the block before the test began was not available but the bottom left corner was intact when the block was purchased. This type of deterioration is typical of that found in the field.

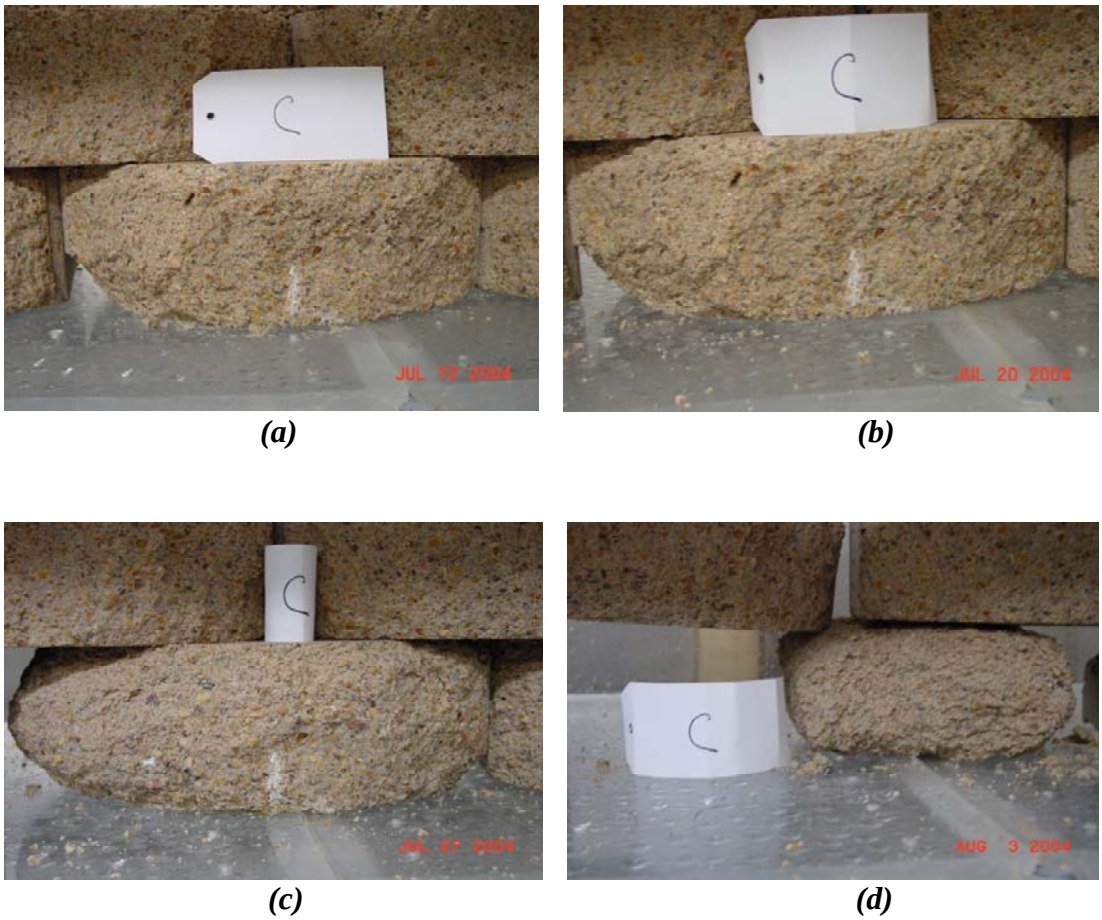

(a) ***(b)***

(c) ***(d)***

Figure 3.15 Freeze-thaw deterioration over forty cycles from Test 1; a) after 10 cycles; b) after 20 cycles; c) after 30 cycles, d) after 40 cycles.

Figure 3.16 shows the condition of the SRW block after forty freeze-thaw cycles before the loose debris was removed. Notice on the bottom layer that the upper blocks are not showing the same degree of damage. Severe freeze-thaw damage exists on

several of the blocks that closely represent typical field damage modes, which was one of the main objectives of this project.

Figure 3.16 Total SRW damage from Test 1 after forty freeze-thaw cycles.

The blocks exposed to 3 percent NaCl solution and an environmental room ramping rate of 0.18°C (0.3°F) per minute are shown in Figure 3.17. The figure shows the initial conditions of the samples before any freeze-thaw cycles were experienced.

Figure 3.17 Initial condition of SRW for Test 2.

No significant damage was observed until after the SRW blocks were exposed to forty freeze-thaw cycles. This delay was expected because of the slower environmental room temperature ramping rate of 0.18°C (0.3°F) per minute. After forty freeze-thaw cycles were completed, two SRW blocks showed substantial damage. These were Blocks A and E-L, which are located on the lower left corner of the wall structure. The damage is indicated in Figure 3.18.

Figure 3.18 Freeze-thaw damage during Test 2 after forty cycles.

Two additional photographs of Block A were taken to show the extent of damage that occurred. Block A exhibited substantial cracking due to freeze-thaw cycles as shown in Figure 3.19. The exact cycle that the block failed was not determined, but failure did occur over a short period. Figure 3.20 shows the remains of Block A after an attempt to move the block was made.

Figure 3.19 Block A shows extensive cracking after 40 freeze-thaw cycles.

Figure 3.20 Complete failure of Block A when removal attempted.

Because Block A exhibited complete failure, a new block was placed in its location so that the experiment could resume. Additional damage did not occur on any other SRW blocks until after sixty freeze-thaw cycles, where Block I experienced complete failure in a similar fashion as Block A. Photographs of Block I's damage is shown in Figure 3.21 and 3.22.

Figure 3.21 Cracking on Block I after 60 freeze-thaw cycles

Figure 3.22 Back bottom edge scaling of Block I.

The experiment was performed for another twenty freeze-thaw cycles (80 total), before the testing was stopped. The results of this experiment indicated that some bias toward the left side of the wall may be present. The reason for this segregation was not determined. However, it has been well established that the microstructure of different blocks are significantly different. The blocks on the left side could have had microstructures that were more susceptible to freeze-thaw damage.

The third experiment also consisted of SRW blocks exposed to fresh water and an environmental room ramping rate of 0.33°C (0.6°F) per minute**.** These blocks were tested in a new test chamber that was constructed so two experiments could be conducted simultaneously. The SRW blocks for Test 3 are shown in Figure 3.23. The SRW blocks were cycled through 100 freeze-thaw cycles and no damage was indicated. This clearly

shows, as has already noted in the literature, that the application of fresh water only has a slight effect on freeze-thaw deterioration.

Figure 3.23 SRW blocks during Test 3 with no indication of freeze-thaw damage.

The final experiment conducted for the proof of concept test occurred at the same time and environmental conditions as Test 3. However, Test 4 contained SRW blocks exposed to 3 percent NaCl solution during each thaw cycle. There was no substantial freeze-thaw deterioration until after fifty cycles were completed. At this time the two blocks that had cut edges (E-L and E-R) showed severe deterioration as shown in Figure 3.24 and Figure 3.25.

Figure 3.24 Block E-L deterioration after 50 freeze-thaw cycles.

Figure 3.25 Block E-R deterioration after50 freeze- thaw cycles.

It is thought that the cut faces caused these blocks to deteriorate at faster rates than the uncut blocks. However, Block B also had substantial freeze-thaw damage as shown in Figure 3.26.

Figure 3.26 Severe cracking of Block B due to freeze-thaw damage during Test 4 after 50 freeze-thaw cycles.

This experiment continued until 90 freeze-thaw cycles were completed. After 90 freeze-thaw cycles Block I also exhibited extensive damage as shown in Figure 3.27.

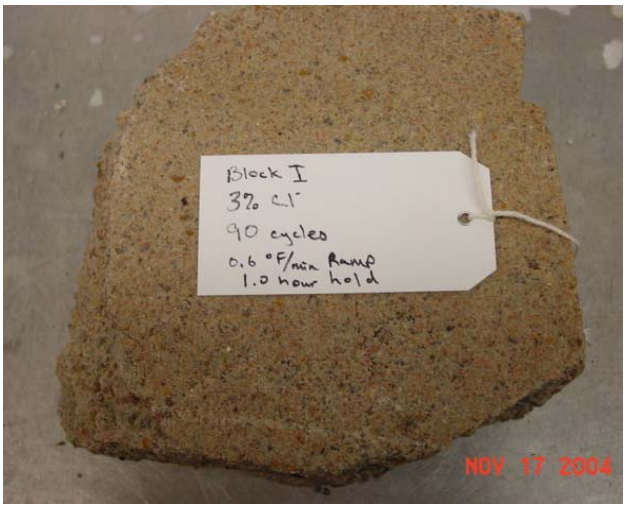

Figure 3.27 Block I exhibiting extensive freeze-thaw damage during Test 4 after 90 freeze-thaw cycles.

3.2.8 Recommendations for Proof of Concept Test

The proof of concept test provided a better understanding of the structure and the components of freeze-thaw testing of SRW blocks. With this, testing parameters such as freeze-thaw cycle times, temperature ramping rates, and NaCl concentration was determined. This experience allowed for several recommendations to be drawn so that preparations for testing larger SRW blocks utilized by SHAs could be made.

Several different environmental room temperature ramping and hold times were evaluated, along with a variation between applying fresh water and a NaCl solution to the SRW blocks. After analyzing the results of each of the experiments performed, it can be concluded that the environmental room ramping rate of 0.55 °C/min (1 °F/min) and the longer temperature hold time is the most detrimental to the SRW blocks freeze-thaw performance. Other rates and hold times also produced freeze-thaw degradation of the

SRW blocks but at slower rates. These slower rates may be more representative of field conditions; however these conditions prolong the testing time.

By observing the SRW blocks as the experiments were conducted, it was observed that the freeze-thaw damage was similar to blocks examined in the field. Typical spalling, scaling, and crack formations were detected on most of the samples. Also, it was determined that exposing the blocks to fresh water during the thaw cycles did not have a notable effect on the integrity of the SRW blocks being tested.

The outcome of the proof of concept test resulted in good correlation with damage of field freeze-thaw specimens. The preliminary proof of concept test indicates that the general test method is likely adequate for evaluating the performance of SRW blocks exposed to freeze-thaw cycles and NaCl.

3.3 PRIMARY TEST

After the proof of concept testing was complete, several SHA approved and non-SHA approved SRW blocks were tested. One modification made to the test setup was an electric heating element typically used for thawing water pipes during winter months, was placed around the PVC pipes when fresh water was applied. Since there was little damage recorded on the proof of concept test with fresh water application, it was thought that the water in the pipes may be freezing and not fully thawing before the water was re-applied.

Also, the temperature hold time during the freeze-thaw cycle was set at two hours instead of one hour to ensure that the center of the SRW blocks were fully frozen and thawed during each cycle. This was important because the blocks being tested in the primary test larger and denser than the landscaping blocks tested in the proof of concept test.

Another change made to the testing procedure before conducting the primary test was the blocks were soaked in the same solution that was sprayed on them during the test before each weighing instead of just being soaked in fresh water. For example, the blocks with NaCl spray exposure during the test was immersed in a 3 percent NaCl

solution before weighing to replenish any moisture loss during the test. However, the blocks exposed to a fresh water spray during the test were immersed in fresh water before weighing. This change was made because it was thought that the denser blocks used in the primary test were losing the NaCl, which had been transferred into the blocks, when soaked in fresh water.

3.3.1 Primary Test Materials

Blocks from three different SRW block manufacturers were evaluated (identified herein as “A”, “B”, and “C”). These blocks, were tested for freeze-thaw durability utilizing the test method developed in this research. Each of these blocks is shown in Figure 3.28, Figure 3.29, and Figure 3.30. Each block type used in the primary test consisted of both SHA approved and non-SHA approved SRW blocks. These blocks vary in geometry and structure, however the SHA approved blocks are required to have a higher strength than the non-SHA approved blocks. The typical dry weight for these blocks is approximately 36 kg (80 lbs). Notice the hollowed out sections in the blocks used for tying the wall structure together.

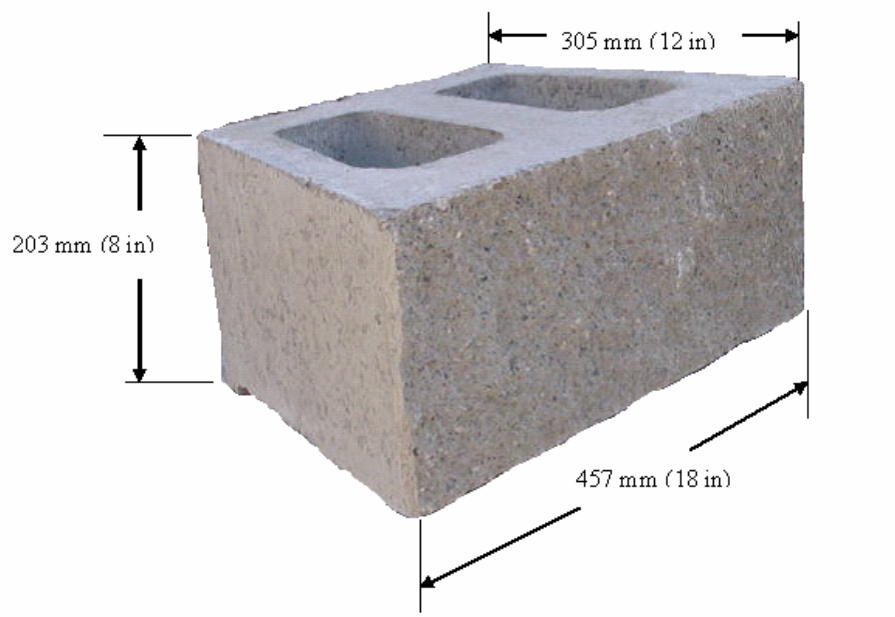

Figure 3.28 SRW block "A".

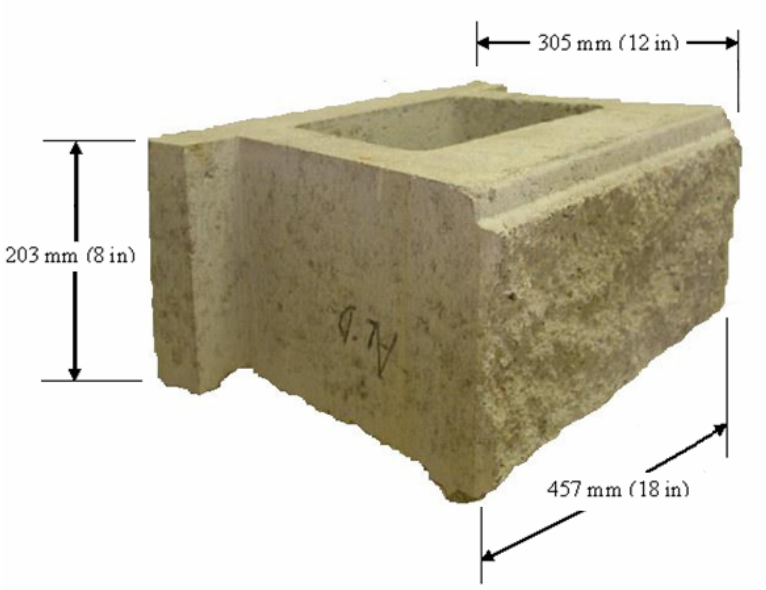

Figure 3.29 SRW block "B".

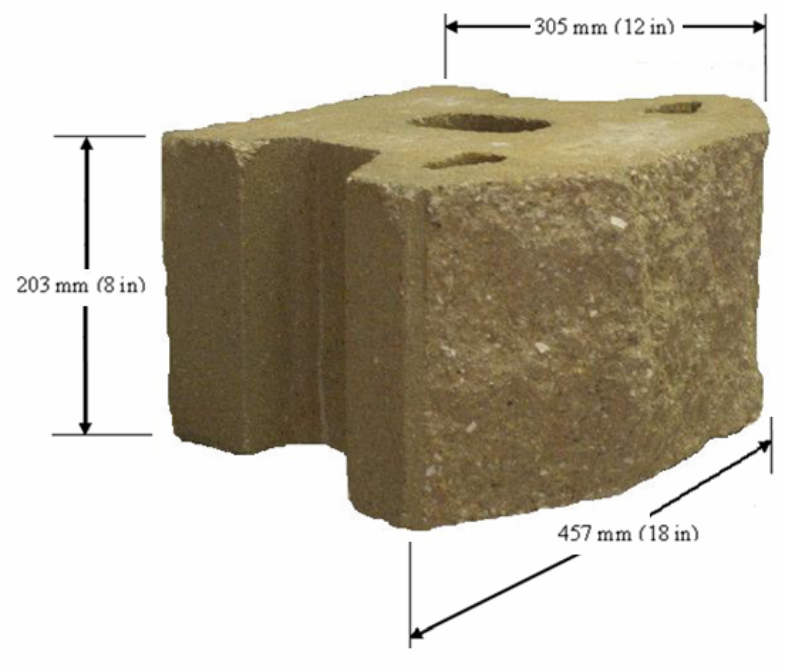

Figure 3.30 SRW block "C".

3.3.2 Primary Test Setup

Each experiment was prepared by separating sets of six SRW blocks. Each block was labeled with a polyvinyl sample tag, which specified the brand, type of block (SHA or non-SHA), solution applied, temperature ramp rate used, location in the test setup, and sample number. The tags were attached to each of the blocks using plastic ties. An example of the labeling method is shown in Figure 3.31.

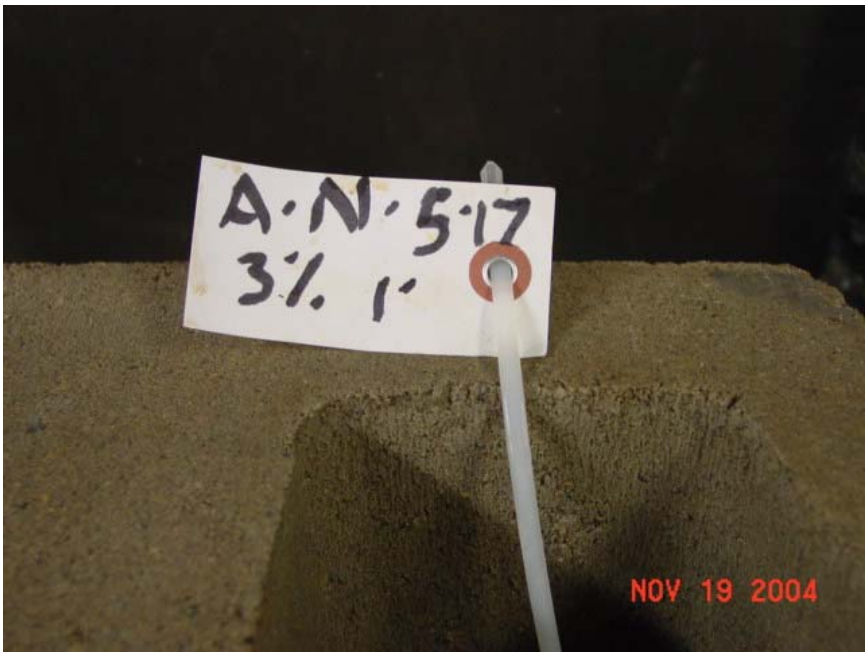

Figure 3.31 Example of SRW block labeling method.

In Figure 3.31, the "A" represents the manufacturer. "N" represents non-SHA approved block, "5" specifies the location that the block was placed during the test, and "17" is the sample number. Also, the "3%" indicates that a 3 percent NaCl solution was applied to this sample, and "1°" indicates that a 0.55°C (1°F) per minute environmental room temperature ramping rate was used. Each of the blocks were then saturated with fresh water or NaCl and weighed. The blocks were placed in their designated test chamber according to their selected position. The positions were numbered 1 through 3 on the bottom row from left to right, and 4 through 6 on the top row from left to right. Only two "A" non-SHA approved cap blocks were available to test. As such, a piece of plexi-glass was placed across the top of each of the of blocks to resemble a row of cap blocks. Then one cap block was placed on the top of the plexi-glass for each test condition to assess their freeze-thaw durability. A typical test setup of each of the three brands of SRW blocks is shown in Figure 3.32, Figure 3.33, and Figure 3.34.

Figure 3.32 SHA approved SRW block test setup with fresh water exposure.

Figure 3.33 SHA approved SRW block test setup with 3 percent NaCl exposure.

Figure 3.34 Non-SHA approved SRW block setup with 3 percent NaCl exposure.

Before the actual test began an SRW block was fixed with a Type J thermocouple to monitor the thermal condition at the center of the block. One thermocouple was placed at the center of the SRW block, while another was used to monitor the environmental room temperature. The thermocouple was placed in the block by first drilling a 6.35 mm (0.25 in) diameter hole approximately 102 mm (4.0 in) to the center of the block at the specified location. The thermocouple was then placed in the hole and backfilled with a mortar mixture paste made from the SRW bock drill dust, cement, and water. One of the blocks used for temperature monitoring is shown in Figure 3.35.

Figure 3.35 Thermal condition assessment setup of SRW block.

The two thermocouples were then attached to a logging thermometer as shown in Figure 3.35. The logging thermometer is capable of recording temperatures from four different channels. Temperatures were recorded every ten minutes during the test to observe the temperature changing rates along with minimum and maximum temperatures. As the freeze-thaw experiments were conducted the temperature was monitored in order to make any changes necessary to achieve freezing and thawing conditions at the center of the SRW blocks. A graph of the typical temperature readings from 20, twelve hour long, freeze-thaw cycles is shown in Figure 3.36.

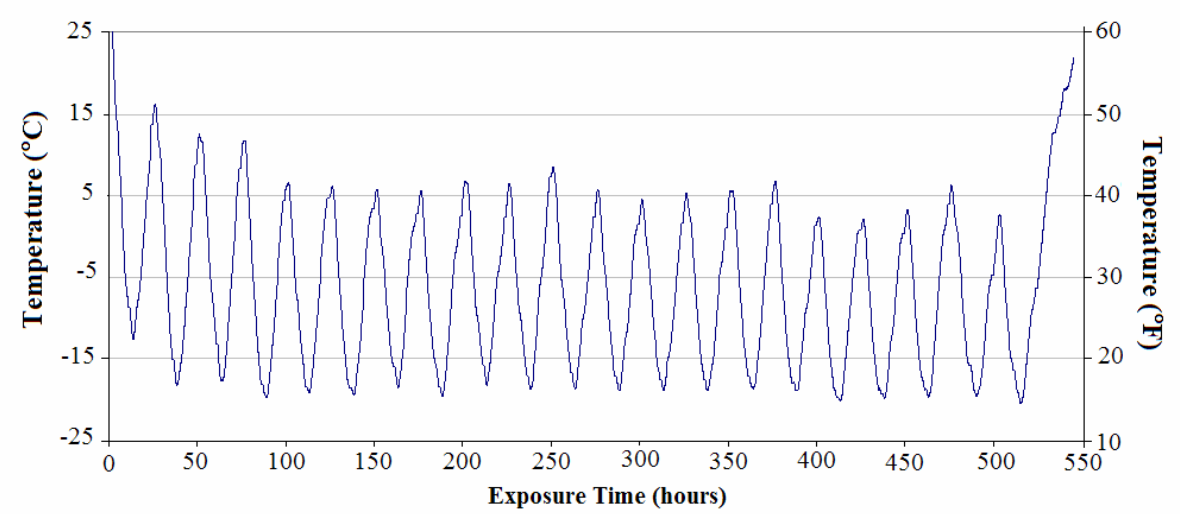

Figure 3.36 Typical temperature data collected for twenty, 12 hour freeze-thaw cycles.

3.3.3 Diffusion Coefficient Determination for Primary Test

Similar to the preliminary test the diffusion coefficient was determined by the test method based on a chloride test developed by the Strategic Highway Research Program (1992). The same method as described in the proof of concept test was used for determining the chloride diffusion coefficient of the SRW blocks used for the primary test. The samples used for the diffusion coefficient experiment were taken from both SHA and non-SHA approved SRW blocks. The samples were removed from the SRW blocks using a coring machine with a 101.6 mm (4 in) diameter coring bit. The samples were cored as shown in Figure 3.37.

Figure 3.37 Coring positions for diffusion coefficient determination.

The cored samples were removed from each of the sides and the back section of the SRW block. These sides were cut by a masonry saw from the block to enable the sections to be placed in the coring machine for a smooth cylindrical cut. Each sample was then coated around the circumference with a low viscosity epoxy. The circular face from the outside of the SRW block was not coated. The samples were then fitted on the non-epoxied side with a 76.2 mm (3 in) long section of clear, acrylic pipe with the inside diameter the same as the cored samples. The samples were then sealed with epoxy to construct a reservoir for ponding. After the epoxy cured, each of the samples were labeled distinguishing the type of block that they were removed from and their location. A photograph of one of the samples is shown in Figure 3.38.

Figure 3.38 Typical diffusion coefficient determination sample.

The label D-BR represents a SHA (D) approved SRW block taken from the back (B), right (R) section of the block. Likewise label N-BL designates a non-SHA (N) approved SRW block taken from the back (B), left (L) section of the block. Each of the reservoirs was filled with a 3 percent NaCl solution and then divided into two groups, the first group included samples N-BL, D-BR, N-L, and D-R. These samples were continuously ponded with the NaCl for three weeks and then removed. The second set of samples included N-BR, D-BL, D-L, and N-R, which were continuously ponded with the same solution for six weeks. Afterwards, the reservoirs were removed from each of the samples and allowed to dry, powder mortar samples were collected at various depths from the front face of the sample using a profile grinder. The mortar dust was collected using a vacuum pump and an aerosol filter system. The standard test method for measuring the total chloride ion content in mortar or concrete using the specific ion probe was used to identify the chloride concentrations at various depths from the face of the

samples. The same calculations were made as in the proof of concept test and the results are reported in the results section.

3.3.4 Mass Loss Determination

The percent mass loss was determined after every twentieth freeze-thaw cycle to record any loss of material from the SRW blocks due to freeze-thaw degradation. Before weighing the samples, each sample was placed in an 83 L (22 gal) rubber storage container with dimensions of 610 x 470 x 508 mm (24 x 18.5 x 20 in) and filled with fresh water or 3 percent NaCl solution. The blocks were saturated for at least twelve hours to replace any moisture lost during testing. The samples were then removed and transported to a weighing station by cart.

The weighing station consists of a reversible load cell with a 15,000 kg (33,000 lb) capacity. The weight of the SRW blocks was determined by placing a metal wire through one of the hollow sections of the block and attaching it to the load cell of the equipment. The scale was zeroed and then each of the blocks was raised until it was free from the base and hanging steady while the weight was recorded to the nearest ±10 g (0.4 oz). After all of the weights were recorded they were entered into a spreadsheet and calculations were made to calculate the percent mass loss of the SRW blocks as a function of the freeze-thaw cycles.

3.3.5 Visual Freeze-Thaw Damage Determination

The SRW blocks were visually inspected periodically throughout each of the tests. Initially and after every tenth freeze-thaw cycle, each block was inspected for freeze-thaw degradation. SRW blocks typically demonstrate freeze-thaw damage through various mechanisms. Some of these means of degradation include popouts, scaling, and cracking. Popouts, small flakes or chips of concrete, are caused by expansion of individual aggregate particles, located near the surface, if saturated during freezing conditions [1]. Scaling is a type of damage that appears as a general deterioration or crumbling of the SRW block in areas that are frequently saturated when exposed to freezing conditions. Cracks may appear randomly on blocks and it is thought

that this is a result of internal microcracking. When these degradation signs were present, photographs were taken of the block and the affected areas. The damaged areas were then monitored for progression of the degradation. The results of the chronological degradation of the SRW blocks was then compiled and compared with the "Distress Identification Manual" developed by Embacher et al. [1]. The basic qualitative damage ranking established by Embacher et al. is:

Severity Levels

Low: Deterioration is localized and minor, exhibiting some *local discoloration* but no significant loss of material.

Medium: Deterioration is present in most areas that might be saturated during freezing and thawing. Discoloration is easily observed and affected areas are exhibiting *tight cracks*.

High: Deterioration is extreme and affected areas are exhibiting *open cracks*.

Each of the SRW block sets were assigned a ranking based on this criteria and results are discussed in the results section.

3.3.6 Internal Cracking Determination

An internal microcrack determination method was developed to analyze representative samples of the SRW blocks. The main objective of this method was to create a technique that could be expanded in future research in order to identify and investigate the damage to SRW blocks from freeze-thaw cycles. The technique developed was based on a dissertation by Nemati [36].

Nemati developed the experimental technique to preserve the compressive stress-induced microcracks in concrete as they exist under applied loads. This technique involves injecting a molten-metal alloy into the induced cracks by applying nitrogen pressure and solidifying it before unloading. Scanning electron microscopy (SEM) was then utilized to capture images from the cross sections of the concrete specimens.

The technique was changed slightly by removing the loading mechanism from the design, because microcracks from freeze-thaw conditions should already be present in the SRW block samples. A simple chamber was designed and constructed to contain the molten metal alloy and the SRW block sample under pressure. The metal was used to fill the pores and cracks in the sample so that a smooth cross section could be obtained and viewed using SEM. The design of the chamber is shown in Figure 3.39 below.

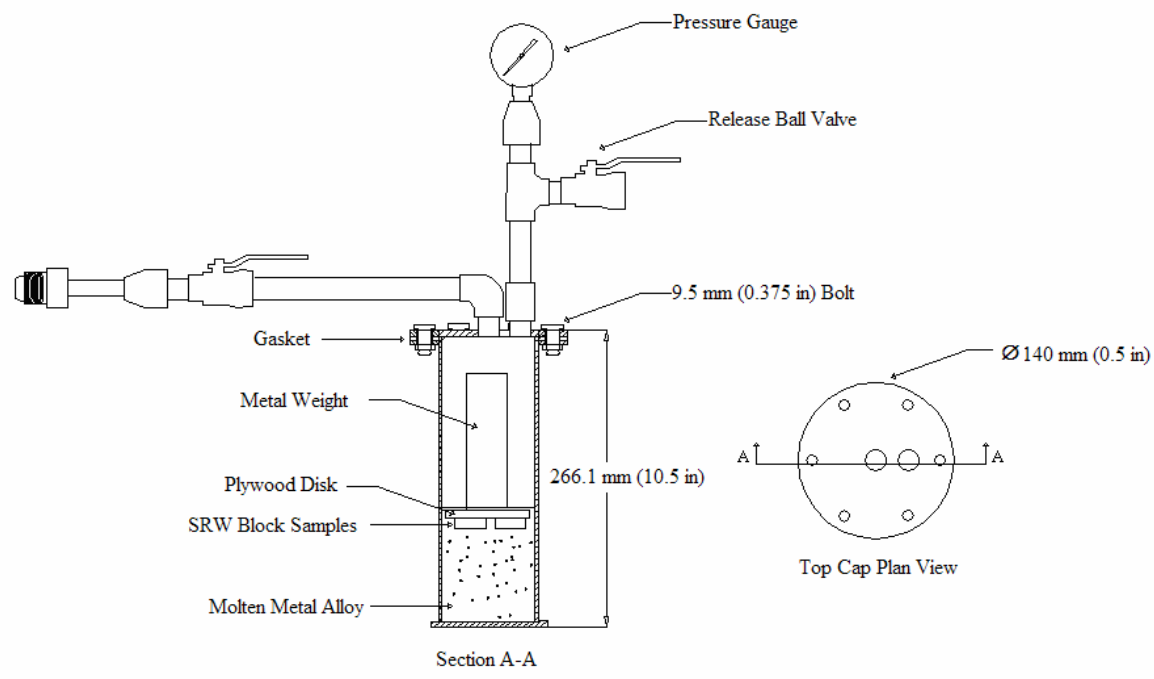

Figure 3.39 Metal injection pressure chamber.

The pressure chamber was constructed with a 76.2 mm (3 in) steel pipe with 3.175 mm (0.125 in) thick walls, 3.175 mm (0.125 in) thick steel plate for the bottom and top flange, and 6.35 mm (0.25 in) thick steel plate for the top cap. The nitrogen flow lines were constructed with 9.53 mm (0.375 in) diameter pipe, fittings, and ball valves. A tightly bounded gasket rated for high pressures and elevated temperatures was used to seal the top cap to the flange. A pressure gauge was fixed to the chamber to monitor the applied pressure to the chamber. The chamber was attached to a cylinder of compressed nitrogen to check for leaks and maximum pressure loading capacity. A photograph of the test setup is shown in Figure 3.40.

Figure 3.40 Internal microcrack determination test setup.

The metal alloy used in this experiment was Cerrosafe™ which is similar to the alloy Wood's Metal, used by Nemati [36]. Cerrosafe™ contains portions of the following metals: Antimony, Bismuth, Cadmium, Copper, Indium, Lead, Silver, Tin, and Zinc. It has a melting point of 85°C (185°F) and is solid at room temperature, which allow the alloy to melt easily, and to readily flow into pores and cracks and while solidify quickly.

The chamber was loaded with 2.27 kg (5 lb) of Cerrosafe™ and melted by placing the chamber on a standard laboratory hot plate. After the alloy was completely melted, representative samples with dimensions of 25.4 x 25.4 x 12.7 mm (1.0 x 1.0 x 0.5 in) of SRW blocks were dried in an oven for twelve hours and then placed into the chamber. Samples of SHA and non-SHA approved blocks that had been exposed to freeze-thaw conditions and those with no exposure where evaluated. The samples floated on top of the molten alloy so a circular cut-out of plywood along with a metal weight was placed on top of them to submerge the samples. The gasket was put in place with a high temperature resistant silicone on both flat surfaces and then the top cap was bolted to the flange. The chamber was then attached to the compressed nitrogen cylinder, while remaining on the hot plate. The chamber was kept on the hot plate for an additional fifteen minutes to ensure that the samples and the molten alloy had reached equilibrium temperatures. The nitrogen cylinder was then opened slowly with both ball valves closed. As the nitrogen cylinder valve was opened the ball valve adjacent to it was opened slowly while monitoring the pressure gauge. The pressure of the chamber was slowly increased and held at a maximum of 6.8 MPa (1000 psi) for ten minutes.

Afterwards the hot plate was turned off and the pressure of the cylinder was released by closing the valve on the nitrogen cylinder and slowly opening the release ball valve adjacent to the pressure gauge on the chamber. The chamber was unattached from the nitrogen cylinder and the top cap unbolted and removed. Each of the samples were then removed from the molten alloy and placed on the table top to allow them to cool.

The next step was to prepare the samples for imaging by first cutting the samples to expose a cross section. This was done using a diamond cutting blade and cleaning them in isopropyl alcohol in a ultrasonic bath. The samples were then cold mounted in

an epoxy mold (31.75 mm (1.25 in) in diameter by 25.4 mm (1.0 in) in depth) typically used in microscope sample preparation. A silicone mold releasing agent was used so the samples could be easily removed from the mold. Two of the representative samples placed in epoxy molds is shown in Figure 3.41.

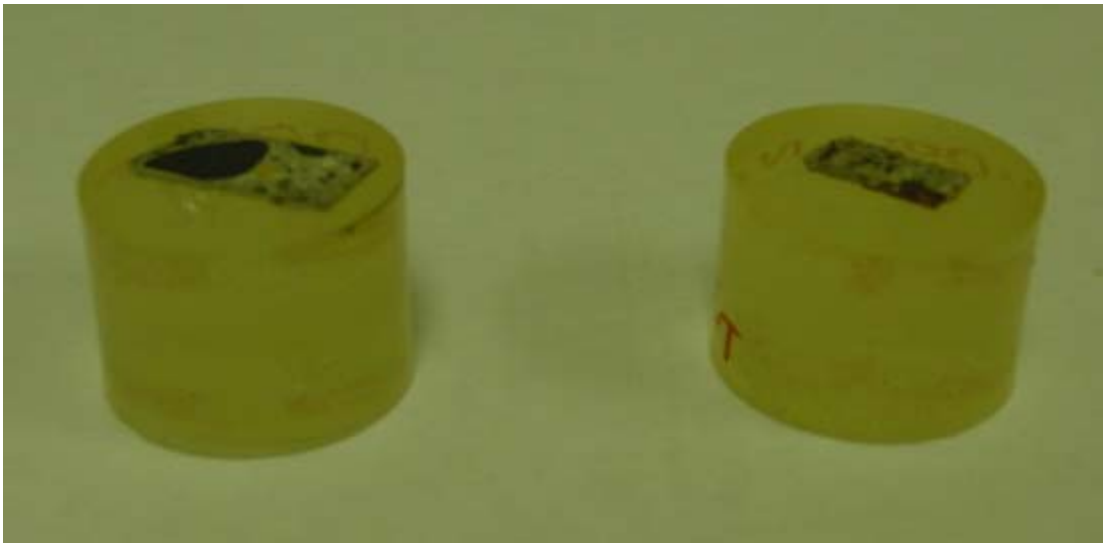

Figure 3.41 SRW samples mounted in epoxy molds for polishing.

After curing, the samples were removed from the mold forms and ground using 400 and 600 silicon carbide papers. After grinding with the 600 grit paper a 6 micron paste was used to further polish the samples. The step was then repeated using a 1 micron paste. The samples were cleaned using distilled water and then studied using a SEM to find microcracks in the SRW blocks.

3.4 FREEZE-THAW TEST PROCEDURE AND EXPERIMENTAL DESIGN

To standardize the new freeze-thaw test method for SRW blocks major steps were identified to conduct the experiment. The steps included the preparation, operation, and decision making stages as shown in the flow chart in Figure 3.42.

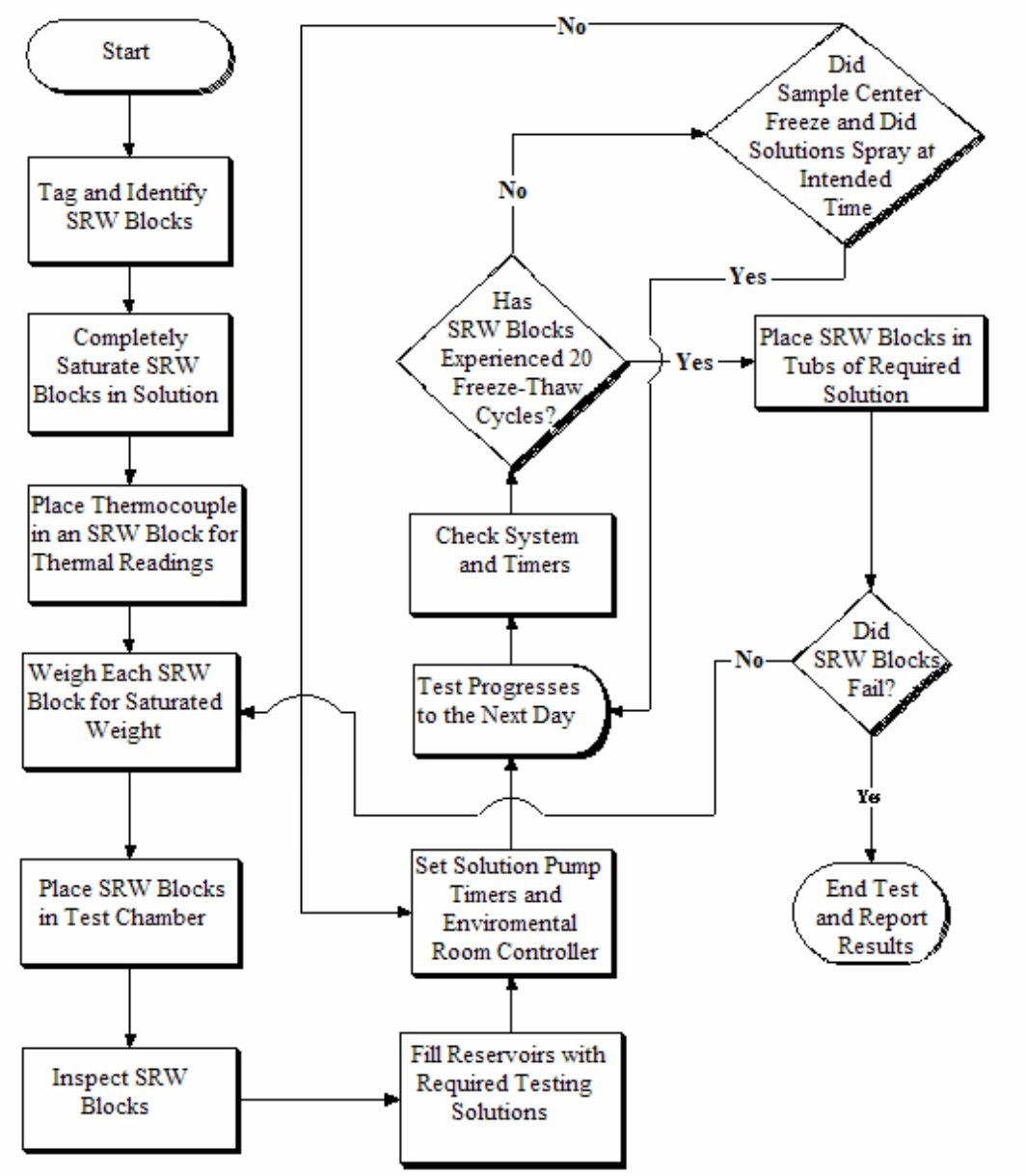

Figure 3.42 Freeze-thaw test procedure flow chart.

The samples to be tested were procured and the amount of testing was, in this work restricted by the number of samples available to the researchers**.** However, it was

anticipated that a good indication of the soundness of this test method was determined. The experiment design is shown in Table 3.3.

Table 3.3 Experimental design matrix of the number of blocks tested.

SRW Blocks Tested	**SRW Block Certification**	**Percent Sodium Chloride Applied**	
		0 percent	3 percent
Block "A"	SHA Approved	6 Blocks	6 Blocks
	Non-SHA Approved	0 Blocks	6 Blocks
Block "B"	SHA Approved	0 Blocks	3 Blocks
	Non-SHA Approved	0 Blocks	3 Blocks
Block "C"	SHA Approved	3 Blocks	3 Blocks
	Non-SHA Approved	3 Blocks	3 Blocks

Additional samples were used for determining the diffusion coefficient. All of the SRW blocks were tested with a 0.55 °C/min (1.0 °F/min) temperature ramping rate and two concentrations of NaCl solutions except for the "B" blocks that were only tested with a 3 percent NaCl solution. The blocks in each test would be determined a failure when the Embacher Severity Level was high.

The freeze-thaw cycle times were adjusted from a six hour cycle to a twelve hour cycle after 160 freeze-thaw cycles were completed on the "B" and "C" blocks. This change was made because it was believed that the inner most water of the blocks may

have not been completely freezing and thawing. If the interior moisture was not completely freezing then the full expansion would not have been experienced, resulting in prolonged testing times.

4. RESULTS AND DISCUSSION

4.1 DIFFUSION COEFFICIENT DETERMINATION

The chloride diffusion coefficients for the primary test were determined using the same method and calculations previously used in the proof of concept test. The diffusion coefficient results are shown in Table 4.1.

The chloride diffusion coefficients of the Non-SHA approved blocks were higher than those of the SHA approved SRW blocks by approximately a factor of two. The mean chloride diffusions coefficients listed in Table 4.1 are comparable to those determined in the proof of concept test. Mean chloride diffusion coefficients for the proof of concept samples are similar to the samples tested here; however, these coefficients decrease as the exposure time increases and in the proof of concept test the coefficients increased. The reason for this is unknown. However one explanation could be that the larger SHA and Non-SHA blocks were younger and still hydrating, thus lowering the diffusion coefficient with time. The smaller SRW blocks may have been older and fully hydrated. Again, these results are several magnitudes higher than that of conventional concrete indicating a more porous material. Therefore, chloride ions are able to be transported more easily through the SRW block structure than that of conventional concrete. Figure 4.1 shows chloride concentration as a function of block depth.

Table 4.1 Chloride diffusion coefficient table.

		Exposure Time	
		3 Weeks	6 Weeks
	Sample	Diffusion Coefficients	
Non SHA Approved	N-L	3.05E-11 m^2/s (4.73E-8 in^2/s)	No Test
	N-R	No Test	6.88E-11 m^2/s (1.07E-7 in^2/s)
	N-BL	9.50E-11 m^2/s (1.47E-7 in^2/s)	No Test
	N-BR	No Test	2.06E-11 m^2/s (3.19E-8 in^2/s)
Mean		*6.28E-11 m^2/s (9.73E-8 in^2/s)*	*4.47E-11 m^2/s (6.93E-8 in^2/s)*
Std. Dev.		*4.56E-11 m^2/s (7.07E-8 in^2/s)*	*3.41E-11 m^2/s (5.29E-8 in^2/s)*
SHA Approved	D-L	No Test	2.15E-11 m^2/s (3.33E-8 in^2/s)
	D-R	3.48E-11 m^2/s (5.39E-8 in^2/s)	No Test
	D-BL	No Test	2.47E-11 m^2/s (3.83E-8 in^2/s)
	D-BR	2.56E-11 m^2/s (3.97E-8 in^2/s)	No Test
Mean		*3.02E-11 m^2/s (4.68E-8 in^2/s)*	*2.31E-11 m^2/s (3.58E-8 in^2/s)*
Std. Dev.		*6.51E-12 m^2/s (1.01E-8 in^2/s)*	*2.26E-12 m^2/s (3.50E-9 in^2/s)*

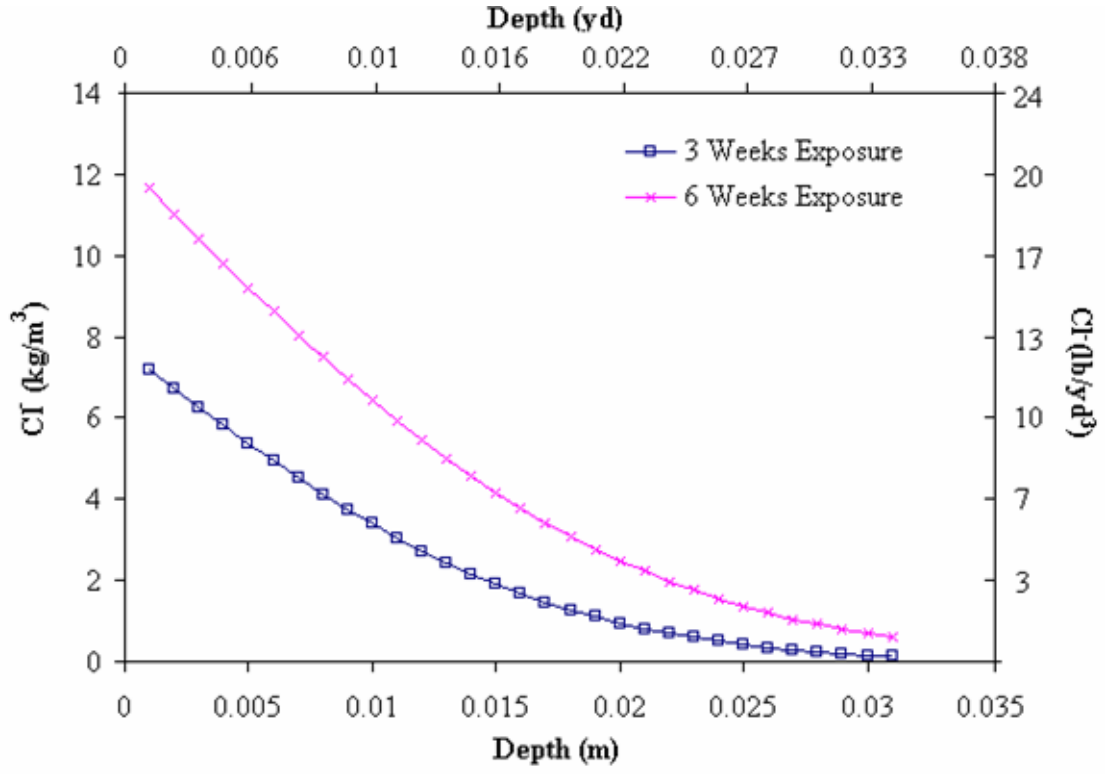

Figure 4.1 Chloride threshold curves for "A" block samples.

4.2 INTERNAL MICROCRACKING DETERMINATION

The main objective of this experiment is to develop and verify a microcrack detection technique that could possibly be used for future research. After representative SRW samples were injected with Cerrosafe™, polished micrographs were obtained to confirm that this evaluation method was feasible. One of the samples studied was not exposed to any freeze-thaw conditions while the other samples were exposed to various numbers of freeze-thaw cycles. Each of the samples was viewed with a microscope to detect microcracks caused by the freeze-thaw exposure. The SRW block sample with no exposure was examined to investigate if there were any initial microcracks in the SRW

blocks resulting possibly from their production process. Figure 4.2 and Figure 4.3 show typical compaction voids with Cerrosafe™. Notice that there are no microcracks present surrounding the voids. Therefore, it is hypothesized that the pressure from the injection process of the metal alloy does not cause microcracks in the samples. The sample was scanned for microcracks and none were identified.

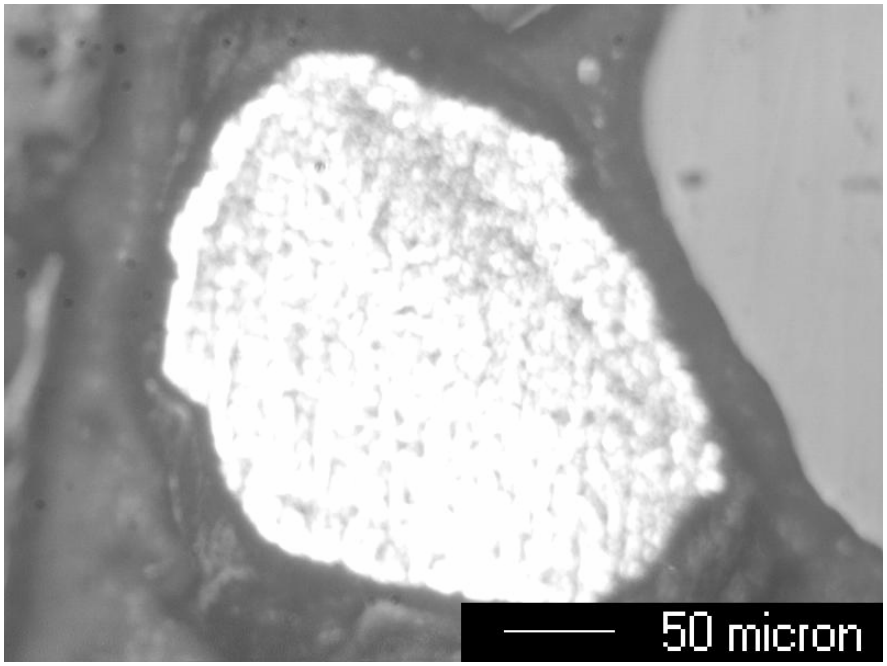

Figure 4.2 Typical compaction void filled with Cerrosafe™.

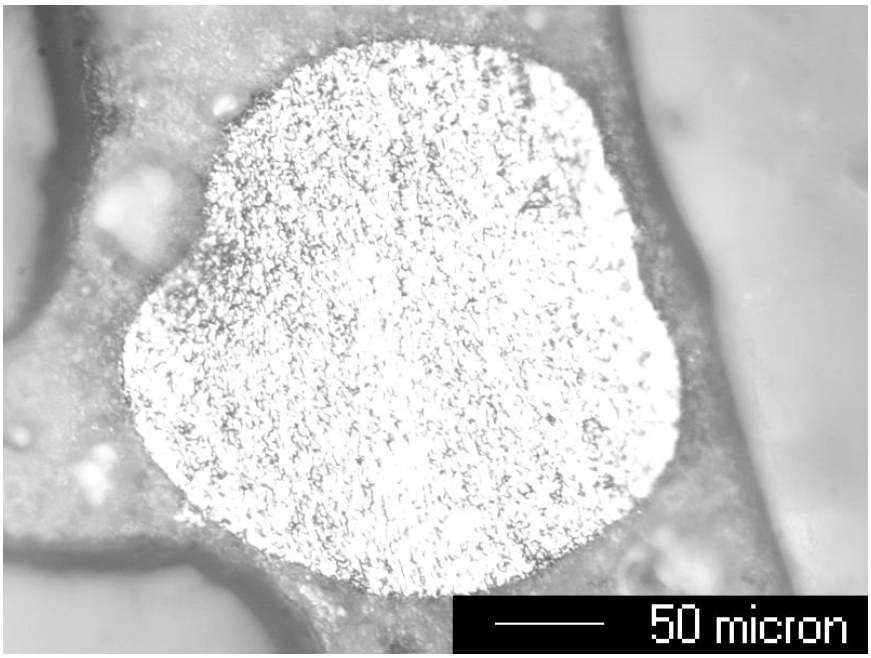

Figure 4.3 Large compaction void filled with Cerrosafe^{TM}.

The two voids in Figure 4.2 and Figure 4.3 are representative of the voids formed during the production process when entrapped air forms in the blocks. These pores are considered macro capillaries with an upper radius of 1 mm (0.04 in). The entrapped air voids are filled with water by means of suction in SRW blocks found in wet environments. When the water-filled entrapped-air voids rapidly reach freezing temperatures the water can not always escape in time before solidifying. The expansion of the frozen water results in the formation of microcracks in the SRW block samples.

The samples that underwent freeze-thaw exposure had multiple forms of cracks extending from the voids within the material. These SRW block samples were also inspected with a microscope to locate any microcracks present caused by freeze-thaw damage.

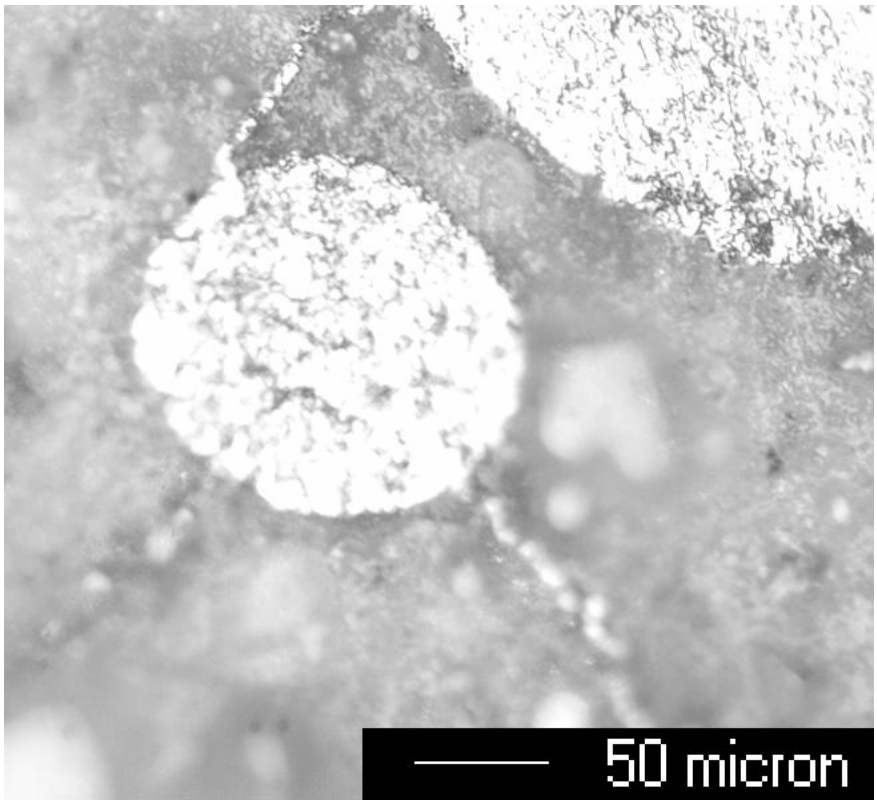

Figure 4.4 Typical void with microcracks spider webbing radially outward.

In Figure 4.4 it can be seen that the microcracks are extending radial outward from the void indicating that hydraulic pore pressure was likely present. The upper right corner of the photograph illustrates a larger compaction void with a microcrack connecting the two voids. This behavior is classic in freeze-thaw microcracking because the cracks tend to propagate through the path of least resistance to relieve the tensile stresses. Similar cracking is shown in Figure 4.5.

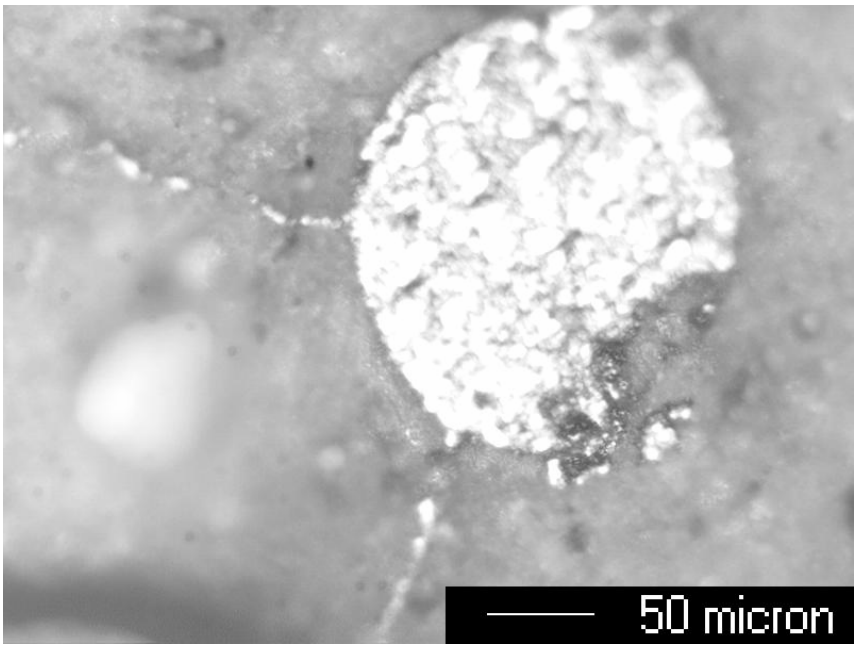

Figure 4.5 Microcracks propagating radially outward from a void from freeze-thaw conditions.

Figure 4.6 and Figure 4.7 illustrate a different potential source of cracking in the structure. These examples show cracks extending from aggregates. A microcrack extending along and radially outward from an aggregate could be caused by the thermal expansion and contraction of the materials present in the concrete (Venecanin 1984). Aggregates usually have different thermal coefficients of expansion than the cement paste surrounding them. When the expansion and contraction rates vary, tensile stresses occur in the cement paste that could cause microcracks. However, it is likely that these microcracks were formed from being exposed to a freeze-thaw environment.

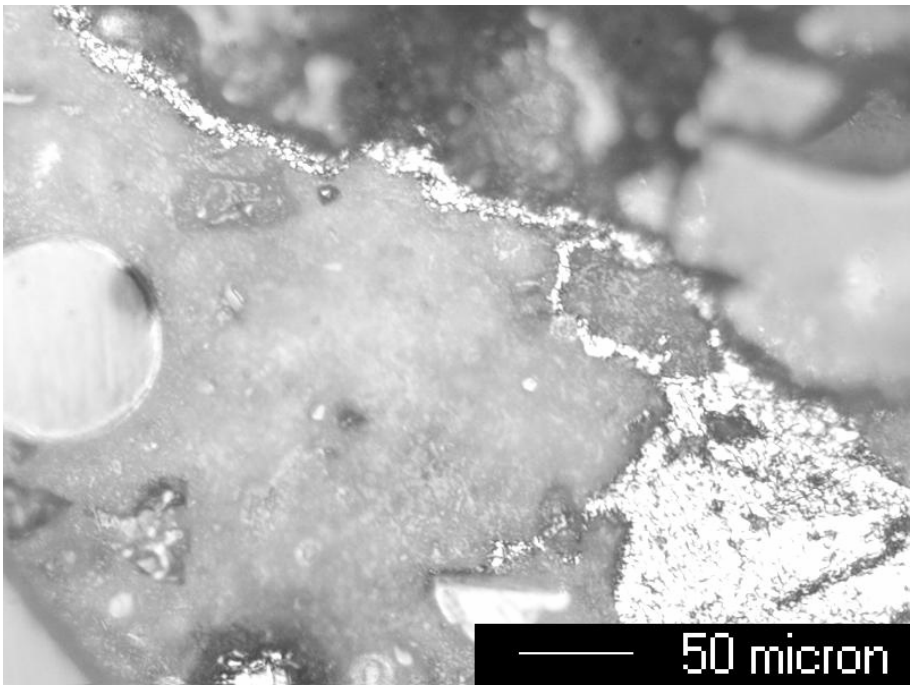

Figure 4.6 Microcracks extending from a void along an aggregate.

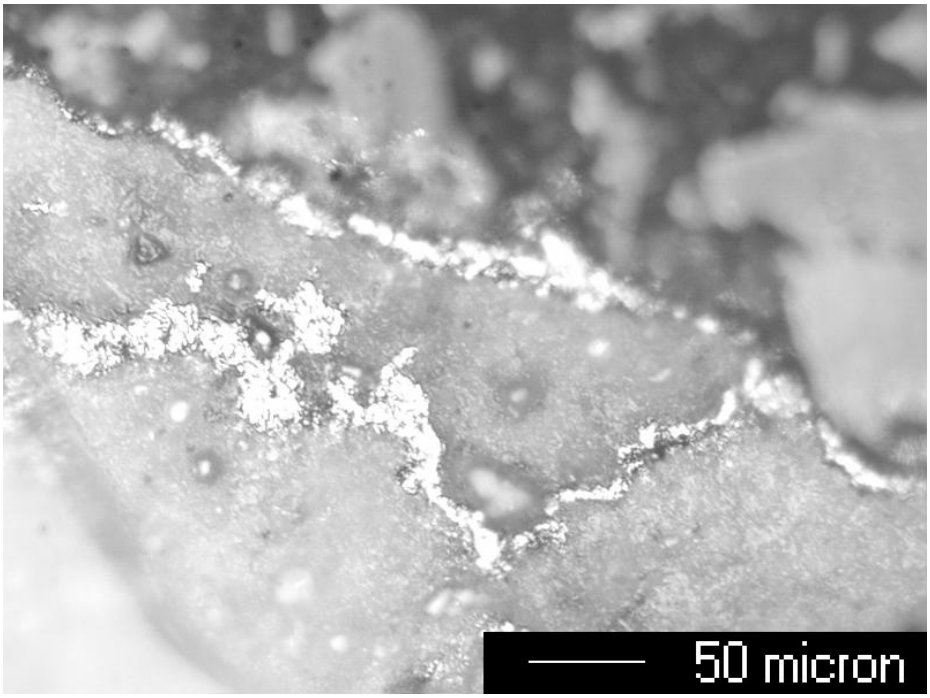

Figure 4.7 A microcrack extending along and radial outward from an aggregate.

The research found that the injection process of the Cerrosafe^{TM} likely does not cause microcracks in SRW blocks. The SRW samples that were exposed to a wet freeze-thaw environment formed microcracks. Entrapped air voids with microcracks forming radially outward are thought to be caused by the internal pore pressure caused by freezing water. The microcracks that formed adjoining the aggregates were likely caused by thermal mismatch between aggregate particles and the paste from freeze-thaw exposure.

The researchers intended to generate discussion for future studies on the microstructure deterioration of SRW blocks and interior degradation due to freeze-thaw conditions. This procedure is likely a good procedure to care out these investigations. An understanding of this mechanism would aid in the estimation of SRW block service life. Also, the process could be beneficial for assessing the integrity of SRWs that have been in service for years. Small samples of the wall can be collected and studied. This internal microcrack identification technique is a prospective tool to future research.

4.3 MASS-LOSS DETERMINATION

The first set of experiments conducted for the primary test consisted of testing two lots of SHA approved “A” blocks and one lot of non-SHA approved “A” blocks. The lot of the SHA approved “A” blocks was sprayed with fresh water during the thawing periods, while the other two lots were sprayed with a three percent NaCl solution during the thawing periods to represent deicing solution exposure along highways. The first sample set tested included six SHA approved “A” SRW blocks that were exposed to a 3 percent NaCl solution along with one Non-SHA approved SRW cap block. Figure 4.8 shows the percent mass loss up to 200 freeze-thaw cycles.

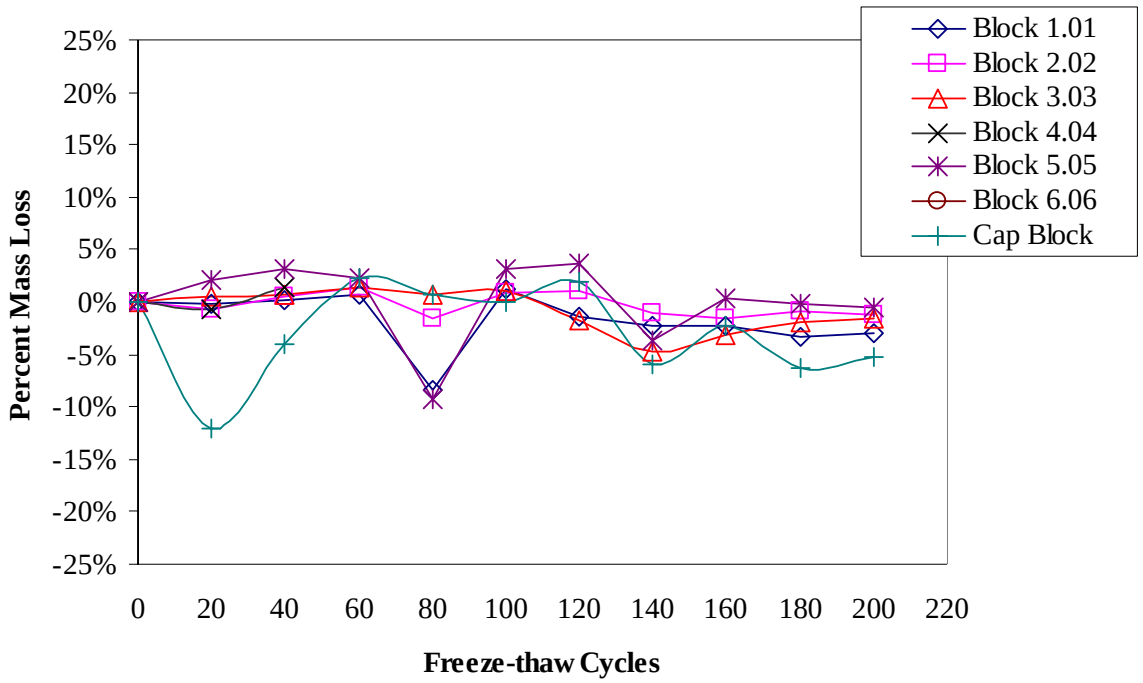

Figure 4.8 Percent mass loss results for SHA approved "A" blocks with 3 percent NaCl solution.

Figure 4.8 indicates that the percent mass loss values for the first set of SRW blocks vary throughout the experiment. This fluctuation is thought to be the result of varying internal moisture conditions of the SRW blocks. The significant reduction of percent mass loss for SRW Bock 4.04 was the result of the sample breaking during a transport. There was no noteworthy mass loss of the remaining samples due to freeze-thaw exposure during this test. The cyclic behavior seen on the Figure 4.8 is believed to be caused by different water saturation levels, likely a result of some microcracking. All blocks were completely immersed in 3 percent NaCl solution for approximately twelve hours with the intention of giving each sample a base condition for weighing. However, even though the surface of each block was dried before weighing of the rough split faces of the blocks retained more liquid than others causing the fluctuating behavior. This behavior was observed throughout all experiments.

The next sample set evaluated was a SHA approved “A” SRW blocks exposed to fresh water during each thaw cycle. The percent mass loss results are revealed in Figure 4.9.

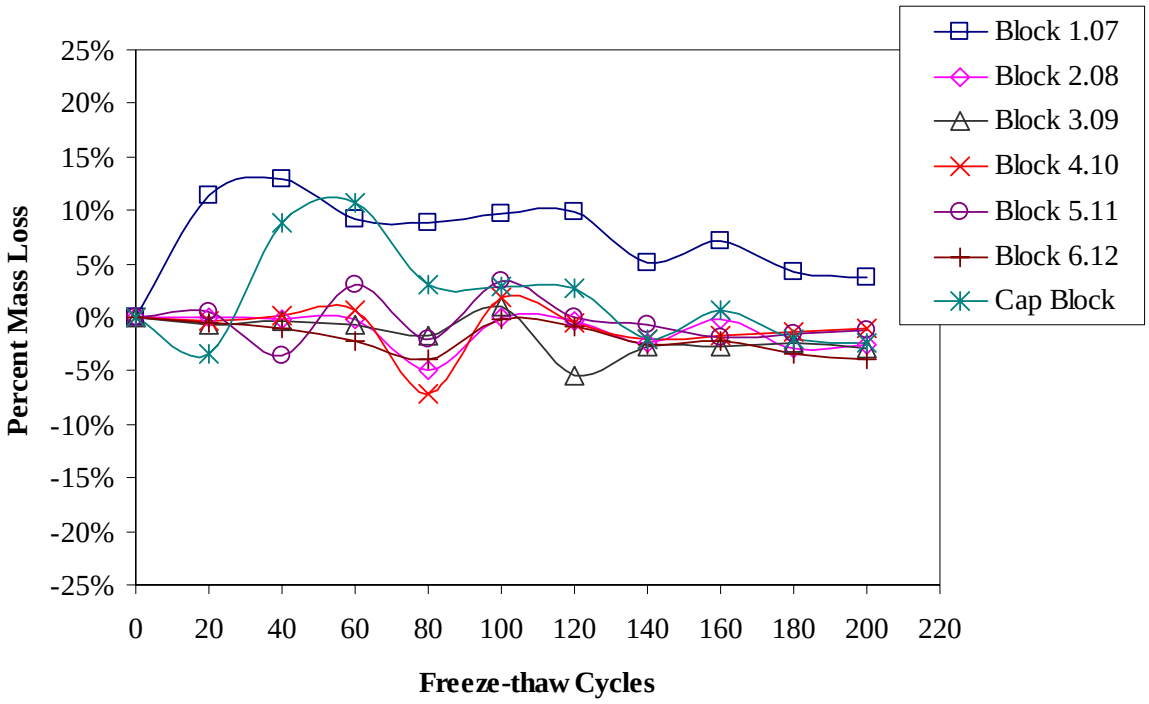

Figure 4.9 Percent mass loss results for SHA approved “A” blocks exposed to fresh water.

Again this cyclic behavior is shown in and there was no significant mass loss due to freeze-thaw cycles. The third set of SRW blocks tested during the first batch of experiments consisted of Non-SHA approved “A” blocks that were exposed to a 3 percent NaCl solution. The percent mass loss results for these samples are presented in Figure 4.10.

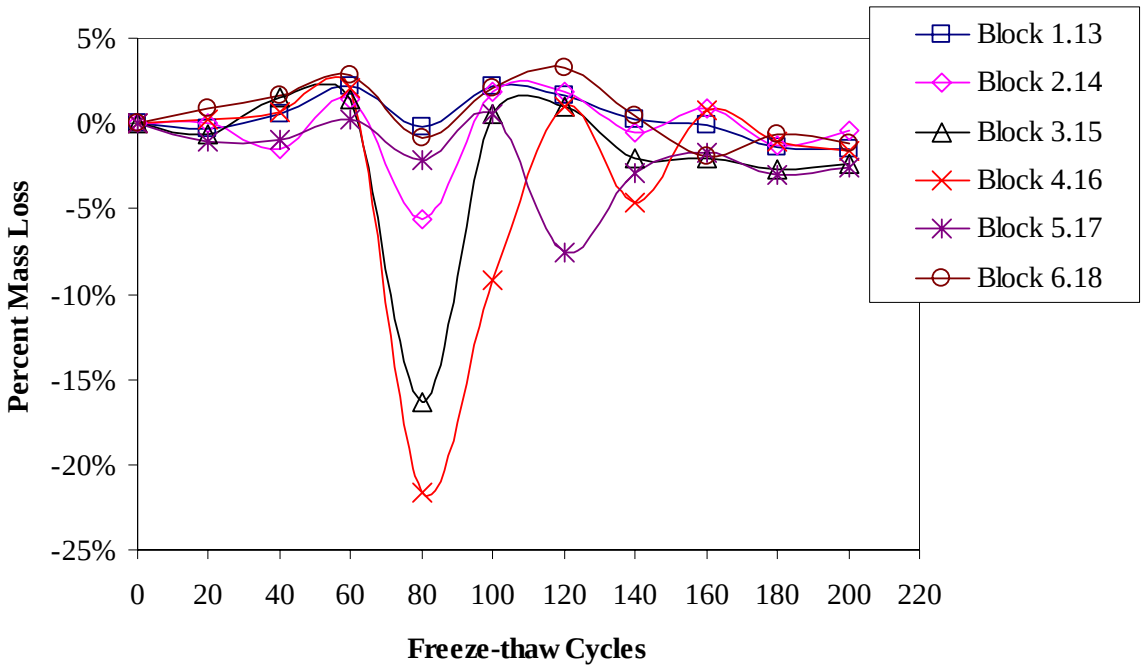

Figure 4.10 Percent mass loss results for non-SHA approved "A" blocks exposed to a 3 percent NaCl solution.

The percent mass loss results shown in Figure 4.10 exhibited non-cyclic mass loss up until cycle 80. Some large oscillations occurred between cycles 80 and 100. The reason for this is unknown.

After 200 freeze-thaw cycles were completed the researchers decided to test two other manufacturers' SRW blocks to differentiate if the freeze-thaw test method would have different results than the "A" blocks. The first set of SRW blocks were a mixture of three SHA approved and three Non-SHA approved "B" blocks exposed to a 3 percent NaCl exposure. The mass loss results for the first set of blocks are shown in Figure 4.11.

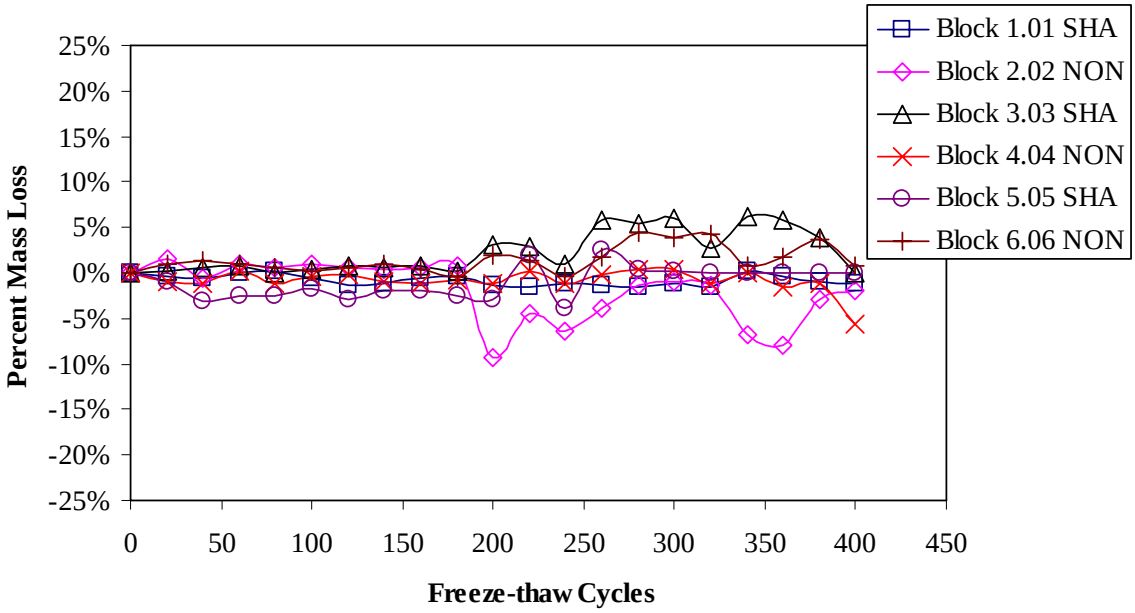

Figure 4.11 Percent mass loss of "B" SRW blocks exposed to a 3 percent NaCl solution.

The percent mass loss results in Figure 4.11 indicate that there was no significant mass loss up until 400 freeze-thaw cycles. The second group of blocks consisted of three SHA approved and three Non-SHA approved "C" blocks exposed to fresh water. These results are shown in Figure 4.12.

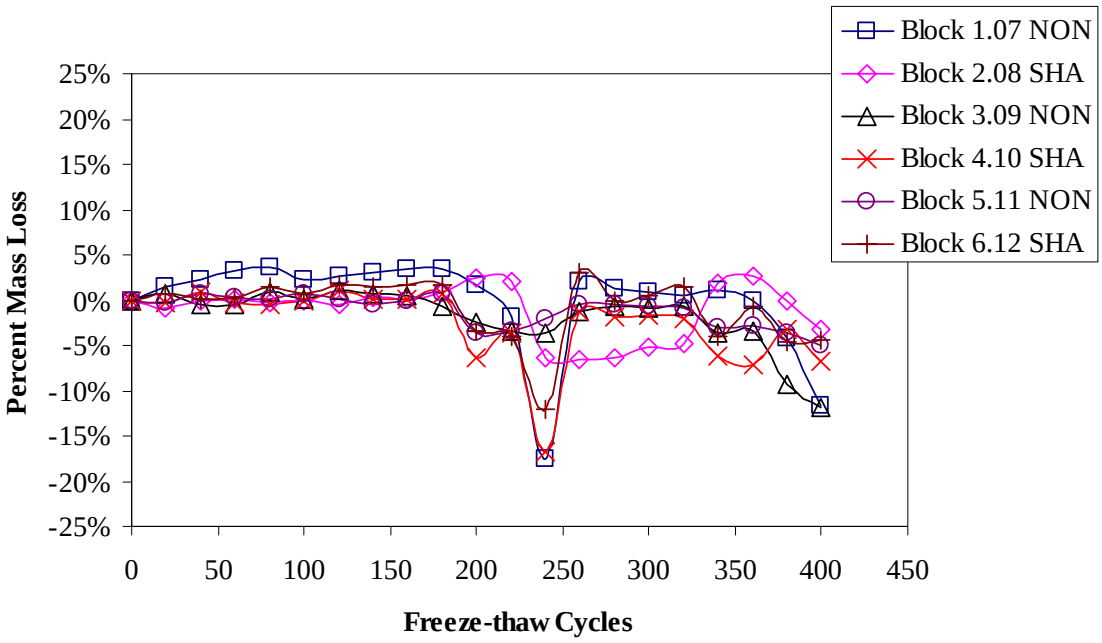

Figure 4.12 Percent mass loss results of SRW "C" blocks exposed to fresh water.

Again three SHA approved and three Non-SHA approved "C" SRW blocks exposed to a 3 percent NaCl solution were evaluated. The percent mass loss results for the last set of samples are shown in Figure 4.13.

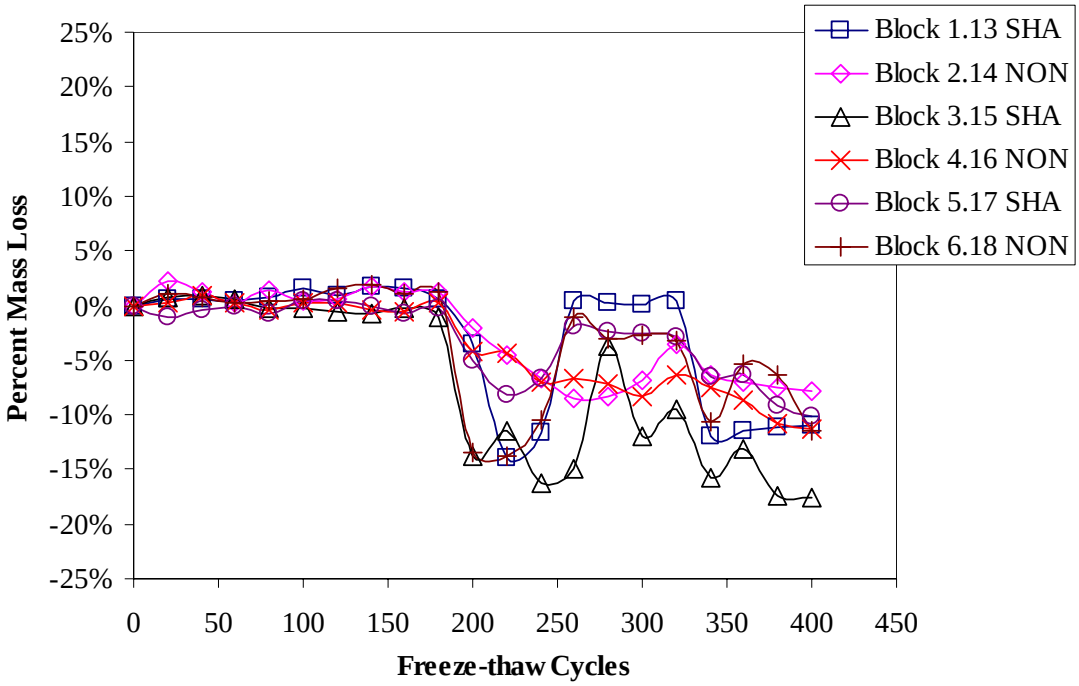

Figure 4.13 Percent mass loss results of SRW "C" blocks exposed to a 3 percent NaCl solution.

These results are similar to the percent mass loss results of the previous test sets in that there was no noticeable mass loss during the duration of the experiment. A common trend between all three groups of blocks is that the percent mass loss of the blocks is constant until 200 cycles were reached. At this point the researchers elected to extend the test cycle time from six to twelve hours. This change was made to study the results of a longer cycle time and to ensure that all of the pore water inside the SRW block would freeze and thaw appropriately.

4.4 VISUAL INSPECTION RESULTS

Along with the block weight data collected every twenty freeze-thaw cycles, photographs were taken of the blocks to record any surface degradation that was present. Representative photographs from each sample after the last freeze-thaw cycle were

obtained. Some samples exhibited minor freeze-thaw damage and others showed no or very little damage.

The first set of SRW blocks exhibited very little freeze-thaw degradation. The Embacher Severity Level assigned to this group of blocks was low. The blocks had some localized discoloration and minor deterioration that accumulated at the bottom of the test setup chamber. Block sample 2.02 is shown in Figure 4.14.

Figure 4.14 SHA approved "A" block 2.02 exposed to a 3 percent NaCl soultion.

The Non-SHA approved "A" cap block that was located in the top center of the assembly of SRW blocks had an Embacher Severity Level of high. This block had severe deterioration of material throughout the surface of the sample.

SHA approved "A" blocks, which were exposed to fresh water, also exhibited a low deterioration level on most of the blocks. However, a few blocks were close to the medium deterioration ranking. Block sample 3.09 in Figure 4.15 represents this condition.

Figure 4.15 SHA "A" SRW block 3.09 exposed to fresh water.

Figure 4.15 clearly shows deterioration at the bottom right corner of the block. However, there were no cracks observed in the block. Again, the non-SHA shown in Figure 4.16 represented a high deterioration level.

Figure 4.16 Non-SHA cap Block "A" exposed to fresh water.

The cap block in Figure 4.16 does not exhibit open cracks, but did before the material separated from the block. However, the rest of the wall blocks in the sample set had a better resistance to the freeze-thaw conditions. Figure 4.17 shows a representative sample from the third set of blocks that were being tested.

Figure 4.17 Non-SHA approved "A" block 6.18 exposed to a 3 percent NaCl solution.

Overall this set of blocks also ranked a low Embacher Severity Level. None of the samples had any cracking or localized deterioration, but some minor discoloration was present. These blocks were exposed to a 3 percent NaCl solution during the thaw cycles. The next set of SRW blocks were exposed to 200 six-hour freeze-thaw cycles and then 200 twelve-hour freeze-thaw cycles. Figure 4.18 shows a representative "B" block.

Figure 4.18 SHA approved "B" block 3.03 exposed to a 3 percent NaCl Solution.

The set of "B" SRW blocks had an Embacher Severity Rating of low to minor medium. In Figure BB there is a small open crack on the lower left face of the block. This is a surface crack that will likely soon release small pieces of block material. There was no differentiation of freeze-thaw damage between the SHA approved and Non-SHA approved blocks with this new test. The crack-like formation on the top center of the block is not from freeze-thaw damage, but was formed during the production process.

The other two sets of blocks tested during the second experiment were "C" SRW blocks. Figure 4.19 shows a representative sample from the set of "C" blocks that were exposed to fresh water.

Figure 4.19 SHA approved "C" block 6.12 exposed to fresh water.

The "C" blocks in this set of blocks had a low freeze-thaw deterioration level. There were only minor areas of discoloration throughout the samples as can be seen on the lower, back corner of Block 6.12 in Figure 4.19.

Figure 4.20 SHA approved "C" block 1-13 exposed to a 3 percent NaCl solution.

The last set of SRW blocks that were tested were exposed to a 3 percent NaCl solution during the thaw cycles. The overall Embacher Severity Level for this set of blocks was low. The block in Figure 4.20 has the top, left corner removed, which was damaged during transportation.

The results obtained from the primary test did not reflect the level of freeze-thaw deterioration that the proof of concept test discovered. The "A" SRW blocks were exposed to both fresh water and a 3 percent NaCl solution during the thaw cycles. The percent mass loss results did not show any substantial material loss throughout 200 freeze-thaw cycles. However, the visual inspections recorded some minor surface damage. The "B" and "C" SRW blocks were exposed to similar conditions for 400 freeze-thaw cycles and no significant mass loss was measured. These tests resulted in a visual inspection Embacher Severity Rating of low to minor medium for Block "B" and

low for Block “C”. Overall the SRW blocks in the primary test did not respond to the freeze thaw conditions they were exposed to.

5. CONCLUSION AND RECOMMENDATIONS

The intent of this project was to develop a freeze-thaw durability test that represents field exposure conditions. The test was developed, modified, and experiments were performed with several different SRW blocks.

5.1 PROOF OF CONCEPT TEST

The proof of concept test was first completed to provide evidence that the procedure could provide representative data of SRW block performance. This test was conducted on small, typical landscaping blocks. The results of this series of tests indicated that the method and parameters used on these SRW blocks can provide representative “field” deterioration for samples undergoing freeze-thaw cycles in a NaCl environment. The failures exhibited during the experiments were similar to typical freeze-thaw failures found in SRW blocks located in the field. There were repeated examples of deterioration and cracking that led to complete block failure. The research indicates that using this test procedure can provide freeze-thaw performance data for these SRW blocks.

5.2 PRIMARY TEST

Because the proof of concept test indicated that the test procedure could provide information on the freeze-thaw performance of small SRW blocks, further studies were performed on larger SRW blocks.

5.2.1 Chloride Diffusion Coefficient Determination

Diffusion coefficients for larger SRW blocks are approximately one to two orders of magnitude larger than conventional concrete. Because salt exposure has been shown to cause rapid deterioration in SRW blocks exposed to freeze-thaw conditions. The faster transport of salts into these blocks can lead to early deterioration.

5.2.2 Internal Microcrack Detection

The main objective of this experiment was to develop a method that could identify microcracks caused y freezing and necessary cycles. Results indicate that the method is easy, feasible, and does identify cracking in SRW blocks exposed to freeze-thaw conditions.

5.2.3 Freeze-thaw Test Method

Testing of larger SRW blocks in the chamber under the conditions of the test procedure failed to clearly distinguish performance levels between SHA approved and Non-SHA approved blocks. The results of these experiments indicated that using this freeze-thaw test procedure and its current parameters is not effective in generating typical field freeze-thaw failures in a timely manner. The prolonged testing time may be contributed to:

1. well designed SRW blocks,
2. larger block mass, and
3. internal block moisture escaping.

These large SRW blocks typically utilized in commercial applications are required to meet higher quality standards than the small SRW blocks used in the proof of concept test. Also, the large, dense blocks may have stronger structural characteristics than the smaller blocks. The internal block moisture, which is the key element in freeze-thaw failure, was thought to have escaped before freezing occurred. This was possibly caused by excessive condensation in the environmental room interfering with the cooling system. With some minor modifications and additional tests, the method developed can present noteworthy freeze-thaw degradation results. However, the testing time to obtain these results is unknown.

REFERENCES

[1] Embacher, R. A., Snyder, M. B. and Shultz, A. E., "Influence of Geographic Location on the Durability of Segmental Concrete Block Retaining Walls Along Roadways."Final Report to Minnesota Department of Transportation. University of Minnesota Department of Civil Engineering. Minneapolis, Minnesota, 2001.

[2] Chan, C., Hover, K., and Folliard, K., "Spatial Variations in Material Properties of Segmental Retaining Wall (SRW) Units, Part 1: Observed Variations," FHWA Project DTFH61-02-R-00078 Quarterly Progress Report, University of Texas, Austin, Texas, 2004.

[3] Haisler, J.P., "Freeze-Thaw Durability of Segmental Retaining Walls", Masters of Science Thesis, School of Civil Engineering, University of Texas, Austin, Texas, 2004.

[4] ASTM C 1262, "Standard Test Method for Evaluating the Freeze-Thaw Durability of Manufactured Concrete Masonry Units and Related Concrete Units," Vol.04.02. American Society for Testing Materials, West Conshohocken, PA, 2004.

[5] Mehta, P.K., and Monteiro, P.J.M., "Concrete: Microstructure, Properties, and Materials," Prentice-Hall, Inc., Englewood Cliffs, New Jersey, 1993.

[6] Setzer, M.J., *Action of Frost and Deicing Chemicals –Basic Phenomena and Testing,* Rilem, London, 1997.

[7] Kosmatka, S.H., Kerkhoff, B., and Panarese, W. C., *Design and Control of Concrete Mixtures,* EB001, 14th edition, Portland Cement Association, Skokie, Illinois, 2002, p.p. 129.

[8] Powers, T.C., "The Air Requirement of Frost-Resistant Concrete," Proceedings, Highway Research Board, Vol. 29, 1949.

[9] Litvan, G. G., "Freeze-Thaw Durability of Porous Building Materials," American Society of Testing and Materials, 1980, pp. 455-463.

[10] Stutzman, P.E., *Freeze-Thaw Damage*, Retrieved February 9, 2005 from the National Institute of Standards and Technology website: http://sftp.cee.uiuc.edu/research/dlange/micro/freeze.html, 2004.

[11] Collins, A.R., "The Destruction of Concrete by Frost," *Journal of the Institute of Civil Engineers,* London, England, Paper No. 5412, 1944, pp. 29-41.

[12] Powers, T.C., “The Physical Structure and Engineering Properties of Concrete,” Bulletin 90, Portland Cement Association, Skokie, IL, 1958.

[13] Venecanin, S.D., "Experimental Study of Thermal Incompatibility of Concrete Components," Proceedings, 3rd RIL EM International Conference on the Durability of Building Materials and Components, VTT, Espoo, Finland, 2000, pp. 510-520.

[14] Fagerlund, G., *Scaling, Absorption, and Dilation of Cement Mortars Exposed to Freezing and Thawing in NaCl Solution*, J. Marchand, et.al. London, 1995.

[15] Verbeck G. and Klieger P., “Studies of ‘Salt’ Scaling of Concrete”, Highway Research Board Bulletin No 150, 1957, pp 1-13.

[16] Studer, W., *Internal Comparative Tests on Frost-Deicing-Salt Resistance*, E & F Spon. London, 1997.

[17] Pigeon, M., and Langlois, M., 1992, “La Durabilite au gel de betons a haute performance, ”Canadian Journal of Civil Engineering, Vol 19, pp. 975-980.

[18] Bilodeau, A. and Malhotra, V.M., “Deicing Salt Scaling Resistance of ConcreteIncorporating Supplementary Cementing Materials: CANMET Research,” Freeze-Thaw Durability of Concrete, 1997, pp 121-156.

[19] Janssen, D.J., Snyder, M.B., *Mass Loss Experience with ASTM C 666: with and without Deicing Salt*, E&FN Spon. London, 1997.

[20] ASTM C 666, “Standard Test Method for Resistance of Concrete to Rapid Freezing and Thawing,” American Society for Testing Materials, West Conshohocken, PA, 2003.

[21] Jacobsen, S. and Sellevold, E.J., “Frost/Salt Scaling and Ice Formation of Concrete: Effect of Curing Temperature and Silica Fume on Normal and High Strength Concrete,” Freeze-Thaw Durability of Concrete, 1997, pp. 93-105.

[22] Ritchie, T. and Davidson, J. J., “Moisture Content and Freeze-Thaw Cycles of Masonry Materials,” *Journal of Materials*, Vol. 3, No. 3, September 1968, pp. 658-671.

[23] Stark, D., “Effect of Length of Freezing Period on Durability of Concrete,” *PCA Research and Development Bulletin RD096T*, Portland Cement Association, Skokie, IL, 1989.

[24] Diamond, S., Guiraud H., Hornain, H., Marchand, J., and Pigeon, M., "The Microstructure of Dry Concrete Products." *Cement and Concrete Research*, Elsevier Science Ltd., 26(3), 1996, pp. 427-438.

[25] Hazrati, K. and Kerkar, A.V., "Freeze-Thaw Durability of Dry Masonry Concrete," 12th International Brick/Block Masonry Conference, Madrid, Spain, 2000.

[26] BRITE project P-2085., "Freeze-Thaw Durability of Concrete Block Paving.", 1993.

[27] Pigeon, M., and Pleau, R., "Durability of Concrete in Cold Climates." *E&FN Spon*, 1995, p. 244.

[28] MacDonald, Kevin A., Lukkarila, M. R., Nelson, T. D., and Gardiner, A. J., "Freezing and Thawing Resistance of Dry Compacted Segmental Retaining Wall Units," Braun Intertec Corporation, Minneapolis, USA, 1999.

[29] MacDonald, K. A., and Lukkarila, Mark R., "Freezing and Thawing Resistance of Dry Compacted Segmental Retaining Wall Units," *Proceedings of the 1st International Conference on Cement Microscopy*, Montreal, Canada, April-May 2005.

[30] Bremner, T. W. and Ries, J. P., "Test of Freeze-Thaw Resistance of Commercially Available Lightweight and Normal Weight Concrete Masonry Mixes Used inSegmental Retaining Wall Units," *Proceedings, 7th North American Masonry Conference*, Univ. of Notre Dame, South Bend, IN, June 2-5, 1996, pp. 822-835.

[31] Bowser, J. D., Krause, G. L., and Tadros, M. K., "Freeze-Thaw Durability of High-Performance Concrete Masonry Units," *ACI Materials Journal*, Vol. 93, No. 4, 1996, pp. 386-394.

[32] National Concrete Masonry Association (NCMA), "Development of a Freeze-Thaw Test Method and Performance Criteria for Concrete Masonry Units and Related Concrete Units. Phase I of NCMA's Freeze-Thaw Durability Research Program," National Concrete Masonry Association, Herndon, VA, July 31, 1996a.

[33] National Concrete Masonry Association (NCMA), "Research Evaluation of the Concrete Masonry Unit Characteristics that Influence Freeze-Thaw Durability. Phase II of NCMA's Freeze-Thaw Durability Research Program," National Concrete Masonry Association, Herndon, VA, July 31, 1996b.

[34] Scott, S. A., "Freeze-Thaw Deterioration of Concrete Masonry Units," University of New Brunswick, April 1996.

[35] SHRP-S/FR-92-110, Condition Evaluation of Concrete Bridges Relative to Reinforcement Corrosion-Volume 8: Procedure Manual, “Standard Test Method for Chloride Content in Concrete Using the Specific Ion Probe”, Strategic Highway Research Program, Washington, DC, 1992, pp. 85-105.

[36] Nemati, K. M., and Monteiro, P. J., “A New Method to Observe Three-Dimensional Fractures in Concrete Using Liquid Metal Porosimetry Technique, *Cement and Concrete Research*, Vol. 27, No. 9, 1997, pp. 1333-1341.

VITA

Aaron Kindall Hoelscher received his Bachelor of Science degree in Applied Physics from Angelo State University in May 2003, and he received his Master of Science degree in Civil Engineering with an emphasis in Construction Engineering and Management from Texas A&M University in December 2006.

Mr. Hoelscher may be reached at the Trejo Research Group, 3136 TAMU, College Station, Texas 77843. His email address is docbar@tamu.edu.